



Calhoun: The NPS Institutional Archive

Theses and Dissertations

Thesis Collection

1990-09

The design of broadband radar absorbing surfaces

Go, Han Suk

Monterey, California. Naval Postgraduate School

<http://hdl.handle.net/10945/30692>



Calhoun is a project of the Dudley Knox Library at NPS, furthering the precepts and goals of open government and government transparency. All information contained herein has been approved for release by the NPS Public Affairs Officer.

Dudley Knox Library / Naval Postgraduate School
411 Dyer Road / 1 University Circle
Monterey, California USA 93943

<http://www.nps.edu/library>

2

NAVAL POSTGRADUATE SCHOOL Monterey, California

AD-A240 521



DTIC
ELECTE
SEP 13 1991
S D D



THESIS

THE DESIGN OF BROADBAND RADAR ABSORBING
SURFACES

by

Go Han Suk

September, 1990

Thesis Advisor:

H. A. Atwater

Approved for public release; distribution is unlimited.

91-10455



91 9 12 072

Unclassified

security classification of this page

REPORT DOCUMENTATION PAGE

1a Report Security Classification Unclassified			1b Restrictive Markings		
2a Security Classification Authority			3 Distribution Availability of Report		
2b Declassification Downgrading Schedule			Approved for public release; distribution is unlimited.		
4 Performing Organization Report Number(s)			5 Monitoring Organization Report Number(s)		
6a Name of Performing Organization Naval Postgraduate School		6b Office Symbol (if applicable) 3A	7a Name of Monitoring Organization Naval Postgraduate School		
6c Address (city, state, and ZIP code) Monterey, CA 93943-5000			7b Address (city, state, and ZIP code) Monterey, CA 93943-5000		
8a Name of Funding Sponsoring Organization		8b Office Symbol (if applicable)	9 Procurement Instrument Identification Number		
8c Address (city, state, and ZIP code)			10 Source of Funding Numbers		
			Program Element No	Project No	Task No
			Work Unit Accession No		
11 Title (include security classification) THE DESIGN OF BROADBAND RADAR-ABSORBING SURFACES					
12 Personal Author(s) Go Han Suk					
13a Type of Report Master's Thesis		13b Time Covered From To		14 Date of Report (year, month, day) September 1990	
				15 Page Count 70	
16 Supplementary Notation The views expressed in this thesis are those of the author and do not reflect the official policy or position of the Department of Defense or the U.S. Government.					
17 Cosalt Codes			18 Subject Terms (continue on reverse if necessary and identify by block number)		
Field	Group	Subgroup	wave absorber, Dielectric material.		
19 Abstract (continue on reverse if necessary and identify by block number)					
<p>There has been a growing and widespread interest in radar-absorbing material technology. As the name implies, radar absorbing materials or RAM's are coatings whose electric and magnetic properties have been selected to allow the absorption of microwave energy at discrete or broadband frequencies. In military applications low radar cross section (RCS) of a vehicle may be required in order to escape detection while a covert mission is being carried on. These requirements have led to the very low-observable or stealth technology that reduces the probability of detection of an aircraft. The design of radar absorbing materials is limited by constraints on the allowable volume and weight of the surface coating, and it is difficult to design a broadband radar absorbing structure in limited volume. This thesis investigates the use of lossy dielectric materials of high dielectric permittivity in multi-layer composites for the production of low radar cross section (RCS). The analysis is done by computing the plane wave reflection coefficient at the exterior surface of the composite coating by means of a computer program which selects layer parameters which determine low reflection coefficients for electromagnetic radiation under constraint of limited layer thickness as well as maximum frequency bandwidth.</p>					
20 Distribution Availability of Abstract			21 Abstract Security Classification		
<input checked="" type="checkbox"/> unclassified unlimited <input type="checkbox"/> same as report <input type="checkbox"/> DTIC users			Unclassified		
22a Name of Responsible Individual H.A. Atwater			22b Telephone (include Area code) (408) 646-3001		22c Office Symbol 62

DD FORM 1473,84 MAR

83 APR edition may be used until exhausted
All other editions are obsolete

security classification of this page

Unclassified

Approved for public release; distribution is unlimited.

THE DESIGN OF BROADBAND RADAR-ABSORBING SURFACES

by

Go Han Suk
Lieutenant , Korean Navy
B.S., Naval Academy Korea , 1983

Submitted in partial fulfillment of the
requirements for the degree of

MASTER OF SCIENCE SYSTEM ENGINEERING IN ELECTRONIC WARFARE

from the

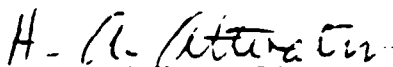
NAVAL POSTGRADUATE SCHOOL
September 1990

Author:

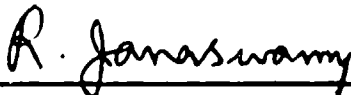


Go Han Suk

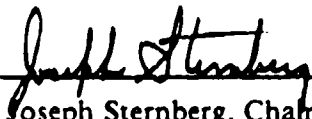
Approved by:



H.A. Atwater, Thesis Advisor



R. Janaswamy, Second Reader



Joseph Sternberg, Chairman,
Department of Electronic Warfare and Anti Submarine Warfare

ABSTRACT

There has been a growing and widespread interest in radar-absorbing material technology. As the name implies, radar absorbing materials or RAM's are coatings whose electric and magnetic properties have been selected to allow the absorption of microwave energy at discrete or broadband frequencies. In military applications low radar cross section (RCS) of a vehicle may be required in order to escape detection while a covert mission is being carried on. These requirements have led to the very low-observable or stealth technology that reduces the probability of detection of an aircraft. The design of radar absorbing materials is limited by constraints on the allowable volume and weight of the surface coating, and it is difficult to design a broadband radar absorbing structure in limited volume. This thesis investigates the use of lossy dielectric materials of high dielectric permittivity in multi-layer composites for the production of low radar cross section (RCS). The analysis is done by computing the plane wave reflection coefficient at the exterior surface of the composite coating by means of a computer program which selects layer parameters which determine low reflection coefficients for electromagnetic radiation under constraint of limited layer thickness as well as maximum frequency bandwidth.

TABLE OF CONTENTS

I. INTRODUCTION	1
II. THEORETICAL ANALYSIS	4
A. IMPEDANCE TRANSFER RELATION FOR LOSSY LAYERS	5
1. MAXWELL'S EQUATIONS	5
2. WAVE IMPEDANCE RATIO OF THE ABSORBER STRUCTURE	9
B. PATTERN SEARCH FOR MINIMUM REFLECTION AT FIXED FREQUENCIES	16
C. PATTERN SEARCH FOR BROAD BANDWIDTH	20
III. RESULTS OF COMPUTATION	22
A. REFLECTION CHARACTERISTICS OF LOW- Γ STRUCTURES DERIVED AT FIXED FREQUENCY	22
B. WAVE-PROPAGATION MODEL FOR LAYER REFLECTION	23
C. SEARCH FOR LAYER STRUCTURES HAVING MINIMUM REFLECTION WITH BROAD BANDWIDTH	34
IV. CONCLUSION	47
APPENDIX A. COMPUTER PROGRAM TO SEARCH FOR MINIMUM REFLECTION COEFFICIENT	49

APPENDIX B. COMPUTER PROGRAM TO SEARCH FOR
 BROAD ABSORPTION BANDWIDTHS 52

LIST OF REFERENCES 55

INITIAL DISTRIBUTION LIST 57

Accession For	
NRIS CR&I	<input checked="" type="checkbox"/>
DTIC TAB	<input type="checkbox"/>
Unannounced	<input type="checkbox"/>
Justification	
By	
Distribution/	
Availability Codes	
Dist	Avail and/or Special
A-1	



LIST OF TABLES

Table 1. INITIAL INPUT PARAMETER VALUES	22
Table 2. RESULTS WITH THE INITIAL PARAMETER VAL- UES FOR FIXED FREQUENCIES	26
Table 3. WAVELENGTH IN STRUCTURE VS. FREQUENCY	28
Table 4. RCS PERFORMANCE OF BROADBAND STRUC- TURES	35

LIST OF FIGURES

Figure 1. NORMAL INCIDENCE OF PLANE WAVE ON A THREE MEDIA STRUCTURE	9
Figure 2. A LINEAR TWO-PORT NETWORK AND ITS ABCD MATRIX	15
Figure 3. FOUR-LAYER ABSORBER STRUCTURE AND ITS PARAMETERS	17
Figure 4. STANDING WAVE IN THE LOSSY STRUCTURE ..	28
Figure 5. STRUCTURE WITH MINIMUM REFLECTION AT 8 GHZ	29
Figure 6. STRUCTURE WITH MINIMUM REFLECTION AT 9 GHz	30
Figure 7. STRUCTURE WITH MINIMUM REFLECTION AT 10 GHz	31

Figure 8. STRUCTURE WITH MINIMUM REFLECTION AT 11	
GHz	32
Figure 9. STRUCTURE WITH MINIMUM REFLECTION AT 12	
GHz	33
Figure 10. BROAD-BAND STRUCTURE RESPONSE	
$(\epsilon_r = 10, 3, 1, 1 \quad \tan \delta = 0.5, 0.5, 0.001, 0.5 \quad l = 2, 3, 2, 3)$	38
Figure 11. NARROW-BAND STRUCTURE RESPONSE DE-	
SIGNED FOR 8 GHz	39
Figure 12. NARROW-BAND STRUCTURE RESPONSE DE-	
SIGNED FOR 9 GHz	40
Figure 13. NARROW-BAND STRUCTURE RESPONSE DE-	
SIGNED FOR 12 GHz	41
Figure 14. BROAD-BAND STRUCTURE RESPONSE	
$(\epsilon_r = 10, 10, 6, 1 \quad \tan \delta = 0.5, 0.5, 0.001, 0.5 \quad l = 2, 3, 2, 3)$	42
Figure 15. BROAD-BAND STRUCTURE RESPONSE	
$(\epsilon_r = 8.5, 10, 6, 1 \quad \tan \delta = 0.5, 0.5, 0.001, 0.5 \quad l = 2, 3, 2, 3)$	43

Figure 16. BROAD-BAND STRUCTURE RESPONSE

$(\epsilon_r = 6, 8.5, 8.5, 1 \quad \tan \delta = 0.5, 0.5, 0.001, 0.5 \quad l = 2, 3, 2, 3) \dots 44$

Figure 17. BROAD-BAND STRUCTURE RESPONSE

$(\epsilon_r = 10, 10, 1, 1 \quad \tan \delta = 0.5, 0.5, 0.001, 0.5 \quad l = 2, 3, 2, 3) \dots 45$

Figure 18. BROAD-BAND STRUCTURE RESPONSE

$(\epsilon_r = 10, 1.9, 1.02, 1.01 \quad \tan \delta = 0.5, 0.5, 0.001, 0.5 \quad l = 2, 3, 2, 3) \dots 46$

ACKNOWLEDGEMENT

I wish to thank my holy God who saves our family and loves us endlessly, and I wish to gratefully express my appreciation to my thesis advisor Dr. H. A. Atwater. He gave a consistent advice and excellent knowledge, professional assistance and moral support throughout this research. Without his assistance, this thesis could not have been undertaken. I am also thankful to professor Ramakrishna Janaswamy for his excellent knowledge and moral support. I would also like to thank to my wife, Mi and daughter, EunBi for their support and patience away from my home during two years of Naval Postgraduate School at Monterey, California.

I. INTRODUCTION

There are continuing requirements for the reduction of the radar cross section (RCS) of military vehicles. Similarly there is a need to reduce the signature of various E.W. systems and payloads attached to these vehicles. The requirements of electronic warfare and electronic countermeasures have been by far the principal motivation for the radar echo reduction of military targets. Electronic countermeasures may take many forms, including passive countermeasures such as target masking or tracker system diversion by clouds of metal particles called chaff. [Ref. 1] The reduction of the intrinsic echo of the target is regarded as a passive countermeasure because no signals are emitted. The purpose of radar absorbing materials (RAM) is to absorb incident radar energy and, thereby, reduce the energy scattered or reflected back to the radar. [Ref. 2] Radar absorbing materials (RAM) play a key role in stealth technology, and their use is a major factor in radar cross section (RCS) reduction. The concept of absorbing incident electromagnetic radiation by placing lossy material in the path of the waves is well established. [Ref. 3]

Despite the recent interest in radar absorbing materials (RAM), initial work on producing practical microwave absorbers dates back before World War II. [Ref. 4] The Jauman absorbers, designed by J. Jauman, were relatively thick (3 inches), being composed of resistive sheets and low-dielectric-constant plastic spacers, and the well known Salisbury screen are early examples. In the 1950s the British Navy compounded ferrites and carbonyl iron to produce a range of absorbers operating at 1-18 GHz. The 1950s also saw much development in the area of broadband anechoic materials. Serious interest by the U.S. Air Force in radar cross section reduction began in 1960s, with most of it being classified in nature. In the late 1970s, the United States began to develop a stealth bomber with low RCS and in the 1990s employed it in an active role.

The applications are numerous particularly at microwave frequencies and include the use of absorbent coatings on the exterior surface of all types of military aircraft and vehicles to reduce radar cross section (RCS). [Ref. 5] If it is assumed that unlimited space is available, the absorption of electromagnetic energy over a wide bandwidth can be obtained by sufficiently increasing the volume of the material and shaping its geometry. But when space is limited, as is normally the case for military ap-

plications, it is a difficult design problem to ensure that the optimal bandwidth and reflectivity properties are achieved to fulfill the requirements for military applications. Constraints on the weight as well as the volume of absorber may exist.

As the name implies, radar absorbing materials reduce the energy reflected back to the radar by means of the absorption of incident electromagnetic energy through ohmic loss in the medium, not unlike the way a resistor dissipates heat when electrical current passes through it. The ideal absorber would be one which allows the incident wave to enter without reflection and then rapidly attenuates the wave to a negligible amplitude in its interior.

Magnetic absorbers involving ferrite compounds have been widely used for operational systems. [Ref. 6] These magnetic absorbers are heavy because of their iron content. [Ref. 7] Hence it is of theoretical interest and practical importance to find a thin non-ferrous absorption structure with low reflection coefficient for electromagnetic radiation. This thesis focuses on the use of lossy dielectric materials to produce low electromagnetic wave reflection at the exterior of a structure with total coating thickness less than 1 cm.

II. THEORETICAL ANALYSIS

In order to minimize the radar signature of a military vehicle using lossy dielectrics with specified scattering properties, which is the task of radar absorbing materials (RAM), the design problem may be considered to be that of achieving a lossy distributed network which matches the impedance of free space to that of the conducting body to be shielded. Radar absorbing materials (RAM) utilize substances which absorb energy from electromagnetic waves passing through them. Such materials have a complex propagation constant in which the imaginary component accounts for the loss in the material. The term loss refers to the dissipation of electromagnetic energy into heat. For many practical electric absorbers, in addition to the loss due to the finite conductivity of the material, there may also be inherent molecular losses.

A plane wave provides a good representation for most of the different forms of wave propagation. [Ref. 8] In a practical sense, electromagnetic waves from any source become essentially plane waves as the distance from the source becomes large. The simplest wave is the uniform plane wave, which is characterized by uniformity of the fields in the plane normal to the direction of propagation and by electric and magnetic fields

which are mutually perpendicular to each other and to the direction of propagation. The present work considers absorption of waves incident normal to the target surface, as a test measure for the electromagnetic absorptivity of the surface structure.

A. IMPEDANCE TRANSFER RELATION FOR LOSSY LAYERS

1. MAXWELL'S EQUATIONS

The basis for the mathematical analysis of the wave phenomena central to this work is the wave equation resulting from Maxwell's equations. [Ref. 9] Maxwell's equations can be manipulated to produce a second order partial differential equation involving only the electric or only the magnetic field. [Ref. 10] The solutions of this equation have the character of electromagnetic waves. Considering wave propagation in a lossy dielectric region, Maxwell's equations become,

$$\nabla \times E = - \frac{\partial B}{\partial t} \quad (2-1a)$$

$$\nabla \times H = J + \frac{\partial D}{\partial t} \quad (2-1b)$$

$$\nabla \cdot E = \frac{\rho}{\epsilon} \quad (2-1c)$$

$$\nabla \cdot B = 0 \quad (2-1d)$$

where ρ and J are volume charge and current densities, and the field vectors have their conventional definitions. Solutions for the field equations are characterized by their vector direction, magnitude and phase. Phasors are, in general complex quantities. For the cases when absorption also needs to be included, i.e. , when medium has a non-zero conductivity or loss tangent, then the dielectric constant can take on complex values. Therefore we consider the behavior of electromagnetic waves in a lossy dielectric region where the conductivity is non-zero. In other words, if the medium is conducting, a current will flow, then equation (2 - 1b) changes to,

$$\nabla \times H = (\sigma + j\omega\epsilon)E = j\omega(\epsilon + \frac{\sigma}{j\omega}) = j\omega\epsilon_c E \quad (2 - 2a)$$

where the effective complex permittivity ϵ_c is defined as,

$$\epsilon_c = \epsilon - j \frac{\sigma}{\omega} \quad (2 - 2b)$$

The other three equations (2 - 1a, c and d) are unchanged. Hence, all the equations for non-conducting media will apply to conducting media if ϵ is replaced by the complex permittivity ϵ_c . When an external time-varying electric field is applied to material bodies, small displacements of bound

charges may result, giving rise to a volume density of polarization. This polarization vector will vary with the same frequency as that of the applied field. As the frequencies increase, the inertia of the charged particles tends to prevent the particle displacement from keeping in phase with the field changes, leading to a frictional damping mechanism that causes power loss because work must be done to overcome the damping forces. This phenomenon of out-of-phase polarization can be characterized by a complex electric susceptibility and an applicable amount of free charge carriers such as the free electrons in a conductor. In treating such media it is customary to include the effects of both the damping and the ohmic losses in the imaginary part of a complex permittivity ϵ_c ,

$$\epsilon_c = \epsilon' - j\epsilon'' \quad (2 - 2c)$$

here both ϵ' and ϵ'' may be functions of frequency. Because conductivity σ of electric absorbers is often the major loss mechanism, it is convenient to include the effects of the conductivity in the term ϵ'' . Alternatively, ϵ'' and σ may be related by an equivalent conductivity representing all losses by writing,

$$\sigma = \omega\epsilon'' \quad (2 - 2d)$$

where ω is the radian frequency. The ratio $\frac{\epsilon''}{\epsilon'}$ is called the dielectric loss tangent because it is a measure of the power loss in the medium and it is customary to write,

$$\tan \delta = \frac{\epsilon''}{\epsilon'} \quad (2 - 2e)$$

This standard procedure leads to the wave equation ,

$$\nabla^2 E = j^2 \omega^2 \mu \epsilon \left(1 + \frac{\sigma}{j\omega\epsilon}\right) E \quad (2 - 3a)$$

Where the complex time dependence $e^{j\omega t}$ has been assumed for all field variables. Then equation (2 -3a) can be reduced to include a complex propagation constant,

$$\nabla^2 E = \gamma^2 E \quad (2 - 3b)$$

Where,

$$\gamma^2 = j^2 \omega^2 \mu \epsilon_c$$

then the complex propagation constant becomes,

$$\gamma = \pm j\omega \sqrt{\mu \epsilon_c} \quad (2 - 3c)$$

2. WAVE IMPEDANCE RATIO OF THE ABSORBER STRUCTURE

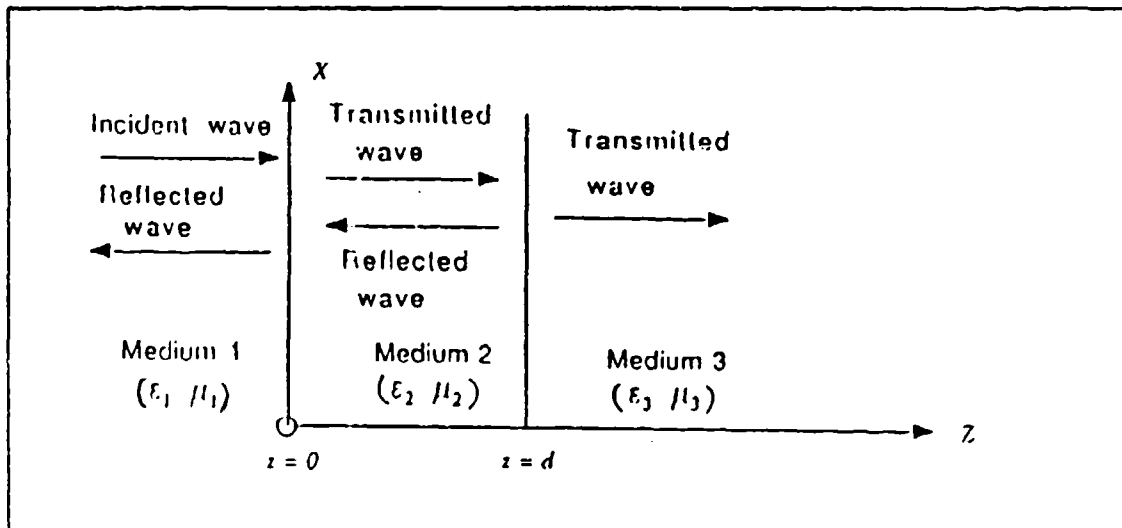


Figure 1. NORMAL INCIDENCE OF PLANE WAVE ON A THREE MEDIA STRUCTURE

Plane waves in the medium are transverse with \vec{E} and \vec{H} perpendicular to each other and to the direction of propagation. The specific surface structure to be investigated is a planar multilayer structure composed of materials having different dielectric properties. As a representative example, consider the three layer structure of general composition shown in Fig.1.

A uniform plane wave traveling in the $+z$ - direction in medium 1 with constants (ϵ_1, μ_1) impinges normally on a plane boundary with medium 2 which has constants (ϵ_2, μ_2) . Medium 2 has a finite thickness and

an interface with medium 3 (ϵ_3, μ_3) at $z=d$. Reflection occurs at both $z=0$ and $z=d$. Assuming an x-polarized incident field, the total electric field intensity in medium 1 can always be written as the sum of the incident component $\vec{a}_x E_{io} e^{-\gamma_1 z}$ and a reflected component $\vec{a}_x E_{ro} e^{\gamma_1 z}$. Then the electric field intensity is given by,

$$E_1 = \vec{a}_x (E_{io} e^{-\gamma_1 z} + E_{ro} e^{\gamma_1 z}) \quad (2-4a)$$

where \vec{a}_x is a unit vector and γ_1 is the propagation constant in medium 1. However, due to the existence of a second discontinuity at $z=d$, the reflected wave amplitude E_{ro} is no longer related to E_{io} as in the case for a boundary between infinite media,

$$E_{ro} = E_{io} \frac{\eta_2 - \eta_1}{\eta_2 + \eta_1} \quad (2-4b)$$

$$\Gamma = \frac{E_{ro}}{E_{io}} = \frac{\eta_2 - \eta_1}{\eta_2 + \eta_1} \quad (2-4c)$$

where Γ is the reflection coefficient for a single boundary, and the η_i are the intrinsic impedances of the respective medium i . Within medium 2, waves bounce back and forth between the two bounding surfaces, some penetrating into regions 1 and 3. The reflected field in medium 1 is the

sum of the field reflected from the interface at $z = 0$ as the incident wave impinges on it, the field transmitted back into medium 1 from medium 2 after a first reflection from the interface at $z = d$, the field transmitted back into medium 1 from medium 2 after a second reflection at $z = d$, and so on. The total reflected wave may be regarded as the resultant of the initial reflected component and an infinite sequence of multiply reflected contributions within medium 2 that are transmitted back into medium 1. The wave impedance of the total field can be defined at any plane parallel to the plane boundary as the ratio of the total electric field intensity to the total magnetic field intensity of the z - dependent uniform plane wave, as was shown in Fig.1. This impedance can be written by,

$$\eta(z) = \frac{\text{total } E_x(z)}{\text{total } H_y(z)} = (j\omega \frac{\mu}{\gamma}) \frac{(E_1 e^{-\eta z} + E_2 e^{\eta z})}{(E_1 e^{-\eta z} - E_2 e^{\eta z})} \quad (2 - 4d)$$

From the definition of propagation constant,

$$j\omega \frac{\mu}{\gamma} = \sqrt{\frac{\mu}{\epsilon_c}} = \eta \quad (2 - 4e)$$

where η is the intrinsic, or wave impedance of the medium. Then, if we place a load impedance at $z = 0$, in Equation (2 - 4d), the wave impedance which results can be written by,

$$\eta_L = \eta_1 \frac{(1 + \Gamma)}{(1 - \Gamma)} \quad (2 - 5a)$$

Where $\Gamma = \frac{E_2}{E_1}$. Then, equation (2 - 5a) can be changed to,

$$\Gamma = \frac{\eta_L - \eta_i}{\eta_L + \eta_i} \quad (2 - 5c)$$

We may find $\eta(l)$ at distance $z = l$ ahead of the termination from the equation (2 - 4d) ,

$$\eta(l) = \eta_i \frac{(e^{\gamma l} + \Gamma e^{-\gamma l})}{(e^{\gamma l} - \Gamma e^{-\gamma l})} \quad (2 - 5d)$$

with the use of equation (2 - 5c) then, the equation (2 - 5d) becomes,

$$\eta(l) = \eta_i \frac{(\eta_L + \eta_i)e^{\gamma l} + (\eta_L - \eta_i)e^{-\gamma l}}{(\eta_L + \eta_i)e^{\gamma l} - (\eta_L - \eta_i)e^{-\gamma l}} \quad (2 - 5e)$$

combining equation (2 - 5e) with the relationships for hyperbolic functions, this equation can be written as,

$$\eta(l) = \eta_i \frac{\eta_L \cosh(\gamma_i l) + \eta_i \sinh(\gamma_i l)}{\eta_L \sinh(\gamma_i l) + \eta_i \cosh(\gamma_i l)} \quad (2 - 5f)$$

where subscript i refers to constants of the i^{th} medium. Here, the complex propagation constant of i^{th} medium is given by,

$$\gamma_i = j\omega\sqrt{\mu_i\epsilon_{ci}} \quad (2 - 5g)$$

and the complex characteristic or wave impedance is ,

$$\eta_i = \sqrt{\frac{\mu_i}{\epsilon_{ci}}} \quad (2 - 5h)$$

As a result, a larger of absorbing material may be analyzed as a section of a transmission line having a characteristic impedance of the form,

$$\eta = \sqrt{\frac{\mu}{\epsilon_c}} \quad (2 - 5i)$$

Where μ is permeability and ϵ_c is the complex dielectric permittivity as,

$$\epsilon_c = \epsilon' - j\epsilon'' \quad (2 - 5j)$$

then, the loss tangent is also defined as,

$$\tan \delta = \frac{\epsilon''}{\epsilon'} \quad (2 - 5k)$$

The loss tangent should be high for rapid attenuation in the line length (or material thickness in this case) and must be chosen to produce given

attenuation. The equivalent circuit for a broadband absorber can be considered as tandem-connected line sections of constant characteristic impedance, composed of lossy elements, or as a transmission line of tapering characteristic impedance such that its input impedance is that of the surface, transforming the impedance of free space, down to a perfect conductor or short-circuit, at the metal backplane.

The radar absorbing structure which was selected for investigation in this work is a planar surface coating composed of separate layers of specified dielectric constants and loss tangents, on a planar substrate assumed to be an ideal conductor. The determination of the radar cross section then reduces to the calculation of the plane-wave reflection coefficient at the exterior surface of the selected laminar coating. The computation of the wave reflection coefficient may be effected on the basis of the direct solution of the plane wave propagation problem in the layer structures. Alternatively, advantage may be taken of the analogy to wave propagation on a system of transmission line sections connected in tandem. In either case, it is useful to represent the successive layers or their transmission-line-segment counterparts in terms of their ABCD matrix characterization as shown in Fig.2. [Ref. 11]

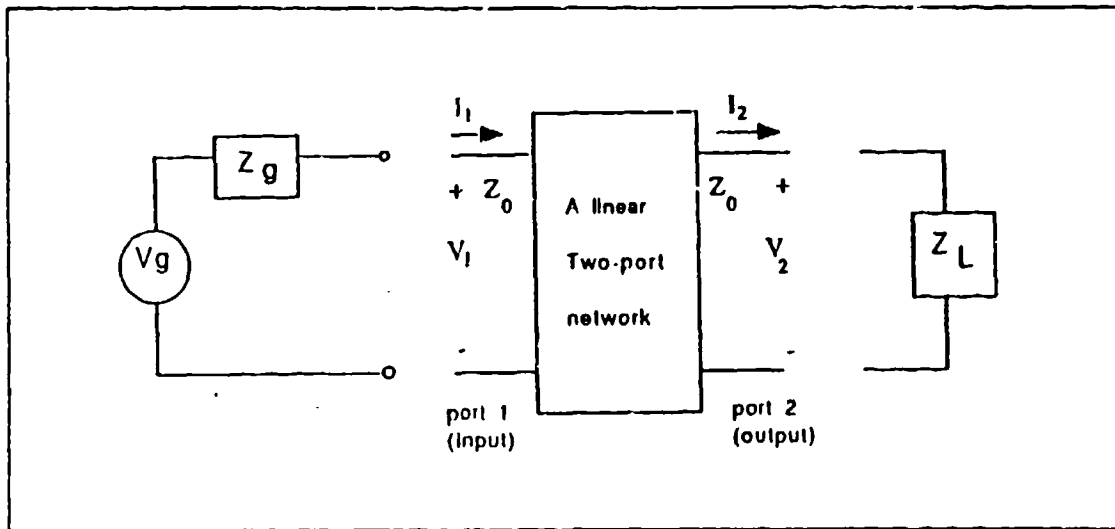


Figure 2. A LINEAR TWO-PORT NETWORK AND ITS ABCD MATRIX

$$V_1 = AV_2 + BI_2 \quad (2-6a)$$

$$I_1 = CV_2 + DI_2 \quad (2-6b)$$

Then the multiplicative property of the ABCD matrices of two-ports connected in tandem may be used to simplify the calculation of the wave propagation in the overall layered structure. The ABCD matrix is a transmission type matrix since in a cascade of two-port networks, the output voltage and current of one network represents the input voltage and current of the following one. So, the expression of the input impedance of a two port in terms of the ABCD matrix is useful in solving impedance matching problems when the output port of the stage is ter-

minated by a load impedance Z_L . For a terminated two - port with load Z_L , the input impedance is given by,

$$Z_{in} = \frac{V_1}{I_1} = \frac{(AZ_L + B)}{(CZ_L + D)} \quad (2 - 6b)$$

The definitions of the parameters are as follows, when the two- port is a line section of length l and propagation constant γ and i^{th} layer impedance Z_i

$$A = \cosh \gamma l \quad (2 - 6c)$$

$$B = Z_i \sinh \gamma l \quad (2 - 6d)$$

$$C = \frac{\sinh \gamma l}{Z_i} \quad (2 - 6e)$$

$$D = \cosh \gamma l \quad (2 - 6f)$$

B. PATTERN SEARCH FOR MINIMUM REFLECTION AT FIXED FREQUENCIES

This method relies on the sequential calculation of input reflection coefficients, with a chosen list of material constants for the successive

layers, in which each solution is compared with the best available up to that time. The parameters of the media of the successive layers are varied in sequence by the program. A scan is made through the selected array of material constants for each medium in turn.

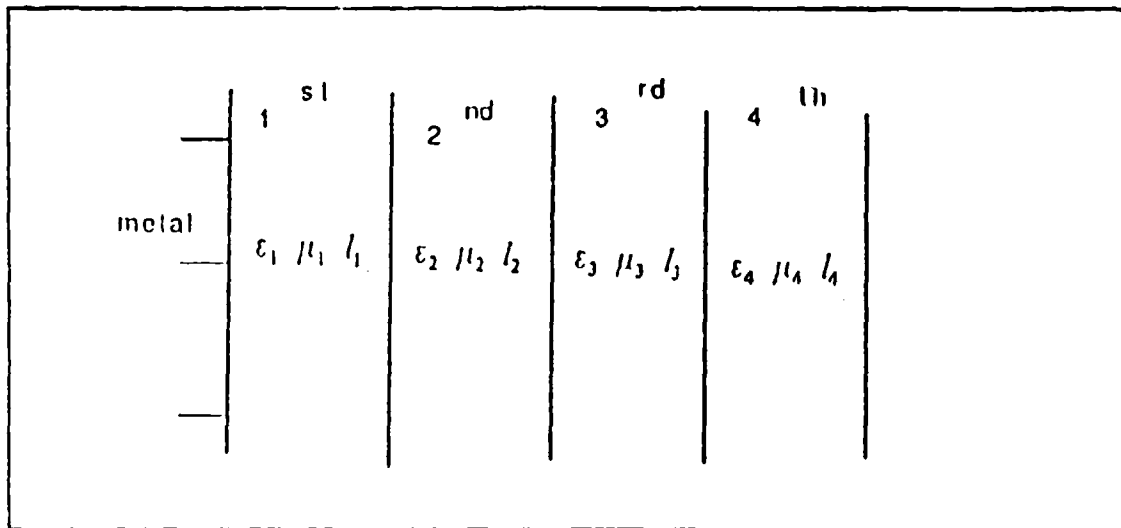


Figure 3. FOUR-LAYER ABSORBER STRUCTURE AND ITS PARAMETERS

Based on practical considerations, an arbitrary choice of a four layered structure was made, each layer having its own value of relative dielectric constant, ϵ_r , its loss-tangent, $\tan \delta$, and its thickness, l . Due to practical considerations, the decision was made to limit the calculation to 5 different values of ϵ_r , 5 different values of $\tan \delta$ and 4 different values of l for the pattern search. Figure 3 shows the four-layer structure with its layer parameters, relative dielectric constant ϵ_r and loss tangent $\tan \delta$.

the selected number of component values, there are $n = 5_s \times 5_s \times 4_s$ ways of composing each layer. Then, the total number of ways of composing the whole four layer structure is $N = (5 \times 5 \times 4)^4$, that is, there are 10^8 different possible compositions for the whole structure. Each of these structures must be tested for its reflection coefficient at the exterior of structure. In order to obtain the desired result we may define an error test function F given by,

$$F = ABS(Z_{in} - 377.0) \quad (2 - 8a)$$

because the impedance of free space is 377 ohm. In order to produce a reflection-free structure the outer surface must be matched to free space. Alternatively, the outer-surface reflection coefficient is given by,

$$\Gamma = \frac{Z_{in} - 377}{Z_{in} + 377} \quad (2 - 8b)$$

The reflection coefficient may be chosen as a test function which has an ideal minimum value of zero. The problem of the calculation of the test-function F of a structure can be separated into two parts. One is the assignment of parameter values to each layer, and the other is the calculation of the ABCD matrix of each successive layer, followed by multiplication of layer matrices to get the final structure matrix. If we consider

that layer(1) is in contact with a metal backplate, then the ABCD matrix parameters can be written as,

$$M_1 = \begin{bmatrix} A_1 & B_1 \\ C_1 & D_1 \end{bmatrix} \quad (2-9a)$$

Consider the next layer matrix to be,

$$M_2 = \begin{bmatrix} A_2 & B_2 \\ C_2 & D_2 \end{bmatrix} \quad (2-9b)$$

In order to get the combined matrix, the foregoing are multiplied to produce the combined matrix,

$$M_{total} = M_2 \times M_1 \quad (2-9c)$$

and sequentially,

$$M_{total} = M_3 \times M_{total} \quad (2-9d)$$

finally,

$$M_{total} = M_4 \times M_{total} \quad (2-9e)$$

In order to find the lowest value of reflection coefficient at the exterior of the structure, the computer program scanned the whole set of structures at a given frequency. The search for the lowest reflection coefficient is performed by comparing each new reflection coefficient value with the previous lowest one (a binary-search method). Then the structure which has the lowest reflection coefficient at a given frequency can be found by the trial.

C. PATTERN SEARCH FOR BROAD BANDWIDTH

In the previous section, the structure which has lowest reflection coefficient value was selected at a given frequency. The investigation showed that the lowest reflection coefficient values were associated with resonant layer structures. These structures typically have low minimum reflection, but with a narrow resonant characteristic. That is, the absorbing range of frequency was excessively narrow. This result occurred because we simply conducted a search to find only the lowest reflection coefficient among structures scanned. In order to identify structures with greater absorption bandwidth, a bandwidth parameter $\Delta\Gamma$ is defined as,

$$\Delta\Gamma = \frac{1}{2} [(\Gamma(f_0 + \Delta f) - \Gamma(f_0)) + (\Gamma(f_0 - \Delta f) - \Gamma(f_0))] \quad (2 - 10)$$

Where f_0 is a frequency of minimum absorption, and Δf is a selected interval. In order to obtain the structures having broad absorption bandwidth, each structure was scanned with changing frequency, while the bandwidth parameter $\Delta\Gamma$ was compared with the previous smaller one. The bandwidth parameter $\Delta\Gamma$ was calculated in the neighborhood of a local minimum reflection coefficient Γ . The lowest value of bandwidth parameter $\Delta\Gamma$ indicates the smallest change of surface reflection for the tested frequency interval, which corresponds to broad absorption bandwidth in radar.

III. RESULTS OF COMPUTATION

A. REFLECTION CHARACTERISTICS OF LOW- Γ STRUCTURES DERIVED AT FIXED FREQUENCY

The objective of RAM design is to produce a material for which the complex reflection coefficient remains as small as possible over a given frequency range. Table 1 shows the initially selected set of parameter values which were employed in the computation of minimum reflection at fixed frequency. The choice of parameters was based on practical considerations of material availability. [Ref. 12]

Table 1. INITIAL INPUT PARAMETER VALUES

Param- eter	Values				
ϵ_r	1.0	3.0	6.0	8.5	10.0
δ	0.001	0.008	0.05	0.1	0.5
$l(mm)$	1.0	2.0	2.5	3.0	-
Fre- quency (GHZ)	8.0	9.0	10.0	11.0	12.0

Using this selected set of parameter values, the work followed a pattern search in order to determine the best structure. In other words, the

problem is to determine what set of layer parameters results in a minimum reflection at the exterior of the coatings with fixed frequency. The fixed frequency scan was performed using the 2-port ABCD matrix form for its convenience as described in the previous chapter. Figure 3 shows the four-layer structure and its layer parameters. The input impedance of the layer in contact with the metal backplane can be taken as,

$$Z_{in1} = \frac{AZ_L + B}{CZ_L + D} = \frac{B}{D} \quad (3 - 1a)$$

since the metal plane can be considered to be a short circuit, i.e. to have zero load impedance ($Z_L = 0$). The use of equations (2 - 6d) to (2 - 6g) then leads to,

$$Z_{in1} = Z_1 \frac{\sinh(\gamma_1 l_1)}{\cosh(\gamma_1 l_1)} = Z_1 \tanh(\gamma_1 l_1) \quad (3 - 1b)$$

B. WAVE-PROPAGATION MODEL FOR LAYER REFLECTION

Consider the four-layer structure in Fig. 3. The input wave impedance to the i^{th} layer is given by,

$$Z_{ini} = Z_i \frac{Z_L \cosh(\gamma l) + Z_i \sinh(\gamma l)}{Z_L \sinh(\gamma l) + Z_i \cosh(\gamma l)} \quad (3 - 2a)$$

where Z_i is the wave impedance of the i^{th} region and Z_L is the terminating load impedance. With the single-layer input wave impedance available, the layers can be cascaded in succession, starting with layer 1 at the metal back plane. Finally, the input impedance to the four-layer structure is,

$$Z_{in4} = \frac{AZ_{in3} + B}{CZ_{in3} + D} \quad (3 - 2b)$$

Since the input impedance of the fourth layer appears at the exterior surface of the structure, the fourth layer input impedance can be considered as the load to the ambient space. Therefore the reflection coefficient under normal wave incidence to the structure can be expressed with the relationship between free space impedance and its load as,

$$\Gamma = \frac{Z_{in4} - Z_0}{Z_{in4} + Z_0} \quad (3 - 2c)$$

Where Γ is the wave reflection coefficient, and Z_0 is the free space impedance of 377 ohms. The reflection coefficient is a complex number since the load impedance is complex. In addition, the reflection coefficient has a magnitude between zero and one from equation (3 - 2c). In discussing the overall reflection coefficient for RCS, it is sufficient to ig-

nore the phase angle and to refer to the amplitude of the reflection coefficient Γ , so the power reflection in decibels can be derived as,

$$\Gamma_p = 20 \log_{10} |\Gamma| \quad (3 - 2d)$$

Thus from equation (3 - 2c), it is seen that zero reflection occurs when the load impedance and the impedance of free space are equal. Finding the lowest reflection coefficient is equivalent to eliminating the difference between the fourth layer input impedance and the impedance of free space. Initially the layer structure parameters were scanned at fixed frequency in order to find the lowest reflection at the exterior of the total structure. Then, the frequency response characteristic, $\Gamma(f)$, for the structure from 1 to 50 GHz was computed. These characteristics are shown in Figs.5 to 9. For each $\Gamma(f)$ curve a polynomial fit of the relative dielectric constant ϵ_r , and loss tangent $\tan \delta$, is shown. These plots of parameter - distribution through those structures having favorable RCS characteristics were constructed in order to provide insight into the characteristics that lead to good RCS performance. Such knowledge will be a useful aid to understanding the mechanism for low RCS. Table 2 summarizes in tabular form the distributions of material parameters, ϵ_r , and $\tan \delta$, which led to the lowest Γ values found at the selected fre-

quencies. As mentioned earlier, the structures which were found to have minimum reflection at fixed frequencies exhibited typically a resonant reflection characteristic.

Table 2. RESULTS WITH THE INITIAL PARAMETER VALUES FOR FIXED FREQUENCIES

Freq (GHZ)	ϵ_r				$\tan \delta \times 10^2$				$l(mm)$				$\Gamma \times 10^3$
	1	2	3	4	1	2	3	4	1	2	3	4	
8.0	10	10	6	6	0.1	0.1	5	50	2	2.5	2.5	3	0.15056
9.0	8.5	10	6	6	0.1	0.8	10	50	2.5	2	2	2.5	0.09035
10.0	3	10	8.5	3	0.8	5	50	50	2.5	2	2.5	3	0.15689
11.0	10	10	10	10	0.1	0.8	0.8	50	2.5	2	1	1	0.02800
12.0	6	8.5	8.5	6	5	10	5	50	2	1	3	1	0.08145

Figs.5 to 9 show that the lowest $\Gamma(f)$ appears at the minimum of a narrow resonant dip in the reflection coefficient of the structure in all cases. The curve of $\tan \delta$ vs. layer - number for these structures demonstrates a characteristic rise in magnitude, in proceeding from the inner layer in contact with the metal to the outer, air-dielectric interface. This means that, with a maximum of conductivity of the medium near the outer surface, there will be a tendency for waves to be trapped within the layer

structure. With lossy media, a trapped standing wave would exhibit a maximum loss at the frequency of resonance for the wave.

Based on the foregoing concept, an average dielectric constant for each entire layer structure was calculated according to definition,

$$\epsilon_{rav} = \frac{\sum_{i=1}^4 \epsilon_{ri} l_i}{\sum_{i=1}^4 l_i} \quad (3-3a)$$

From the this average ϵ_r , the number of wavelengths in the equivalent medium was calculated for each of the resonant frequencies in Figs.5 to 9, according to the expression,

$$N_\lambda = D \frac{f}{c} \sqrt{\epsilon_{rav}} \quad (3-3b)$$

Where $D = \sum_{i=1}^4 l_i$ is the total thickness, and c is the velocity of light in vaccum. The results of this calculation are shown in Table 3. It may be seen that in all cases, the total layer structure thickness amounted to approximately (3,4) wavelengths. In a simple resonance picture, this would correspond to a standing wave distribution with a zero of E field at the metal surface, a node within the material, and a standing-wave maximum

at the air- dielectric interface. This situation is shown schematically in Fig.4. Further analysis has revealed that the narrowband behaviour exhibited in Figs.5 to 9 is due to the gradual variation of the loss tangent parameter. We will see later that to get a broadband response, the loss tangent must be more or less uniform through out the layers.

Table 3. WAVELENGTH IN STRUCTURE VS. FREQUENCY

Freq(GHz)	Wavelengths in structure
8	0.745
9	0.744
10	0.801
11	0.754
12	0.763

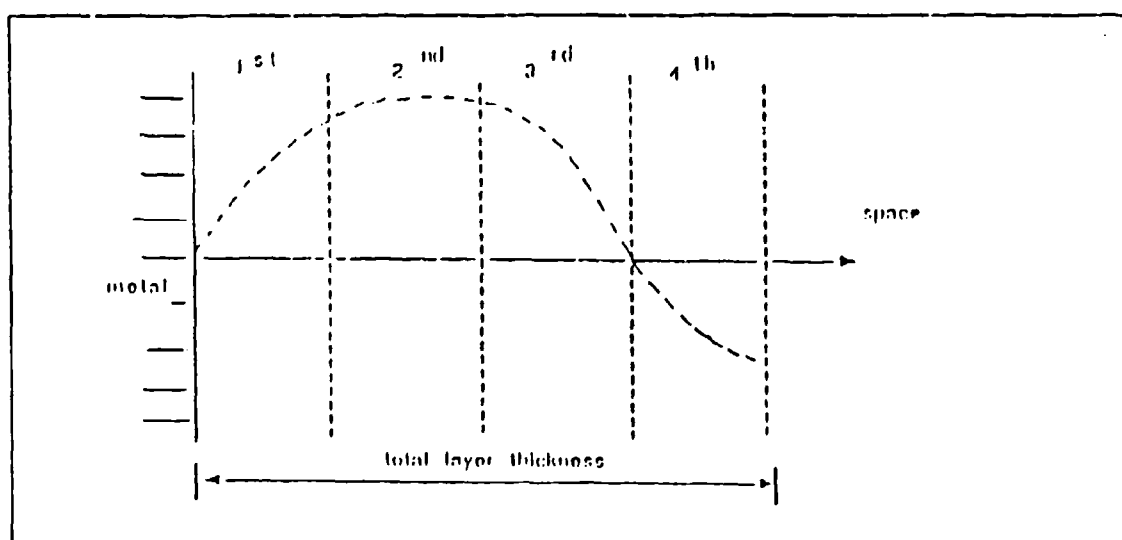


Figure 4. STANDING WAVE IN THE LOSSY STRUCTURE

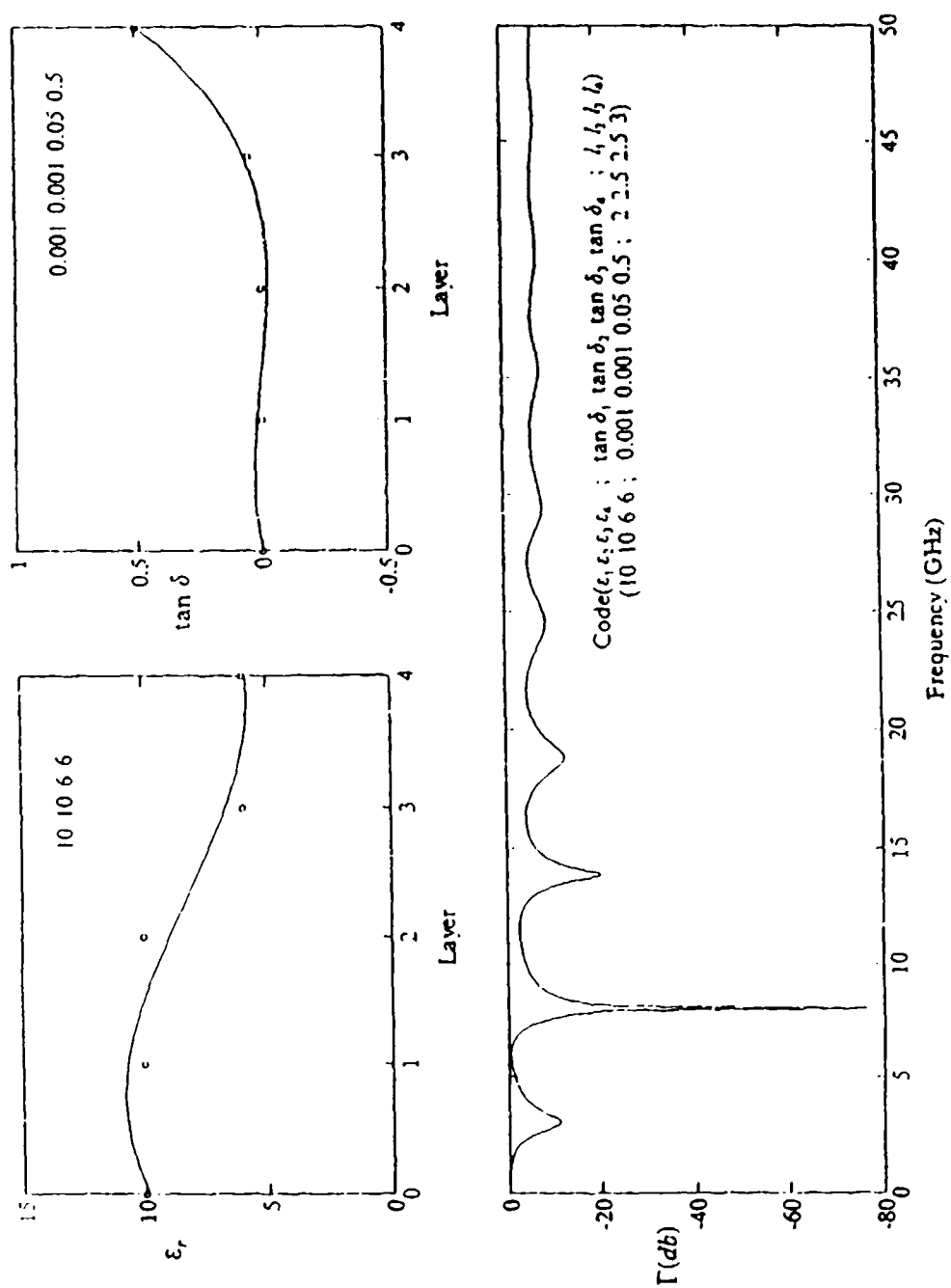


Figure 5. STRUCTURE WITH MINIMUM REFLECTION AT 8 GHz

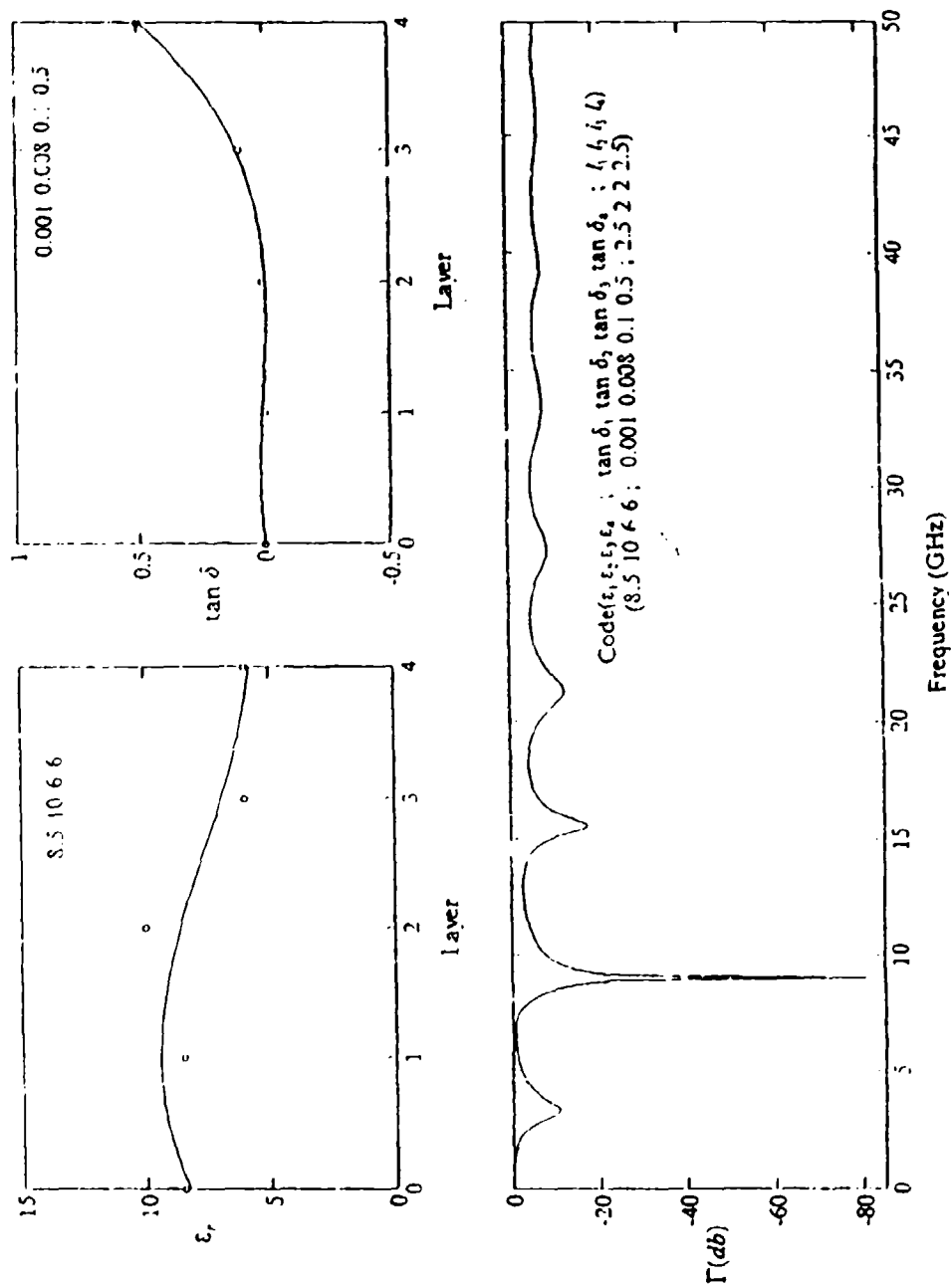


Figure 6. STRUCTURE WITH MINIMUM REFLECTION AT 9 GHz

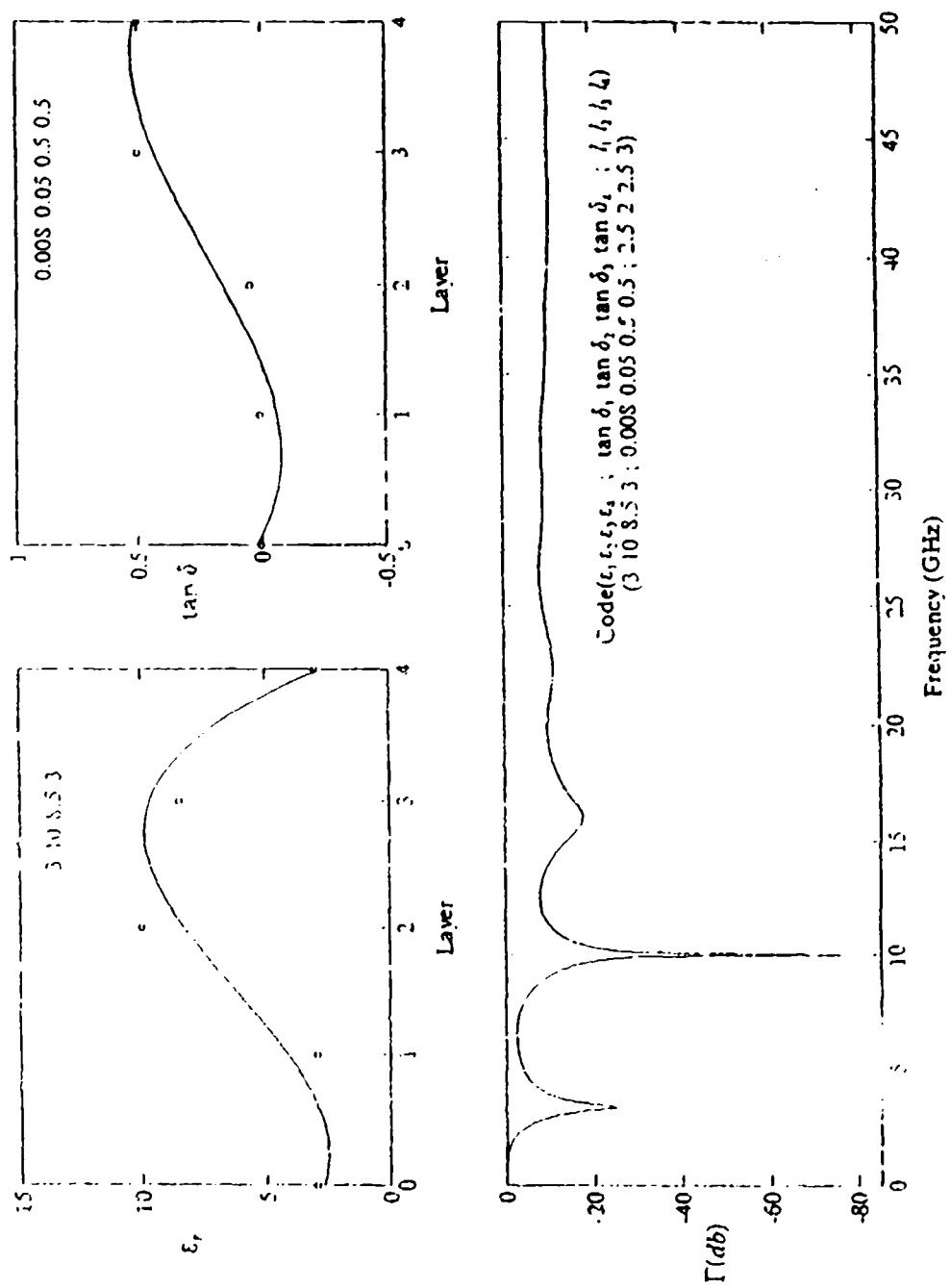


Figure 7. STRUCTURE WITH MINIMUM REFLECTION AT 10 GHz

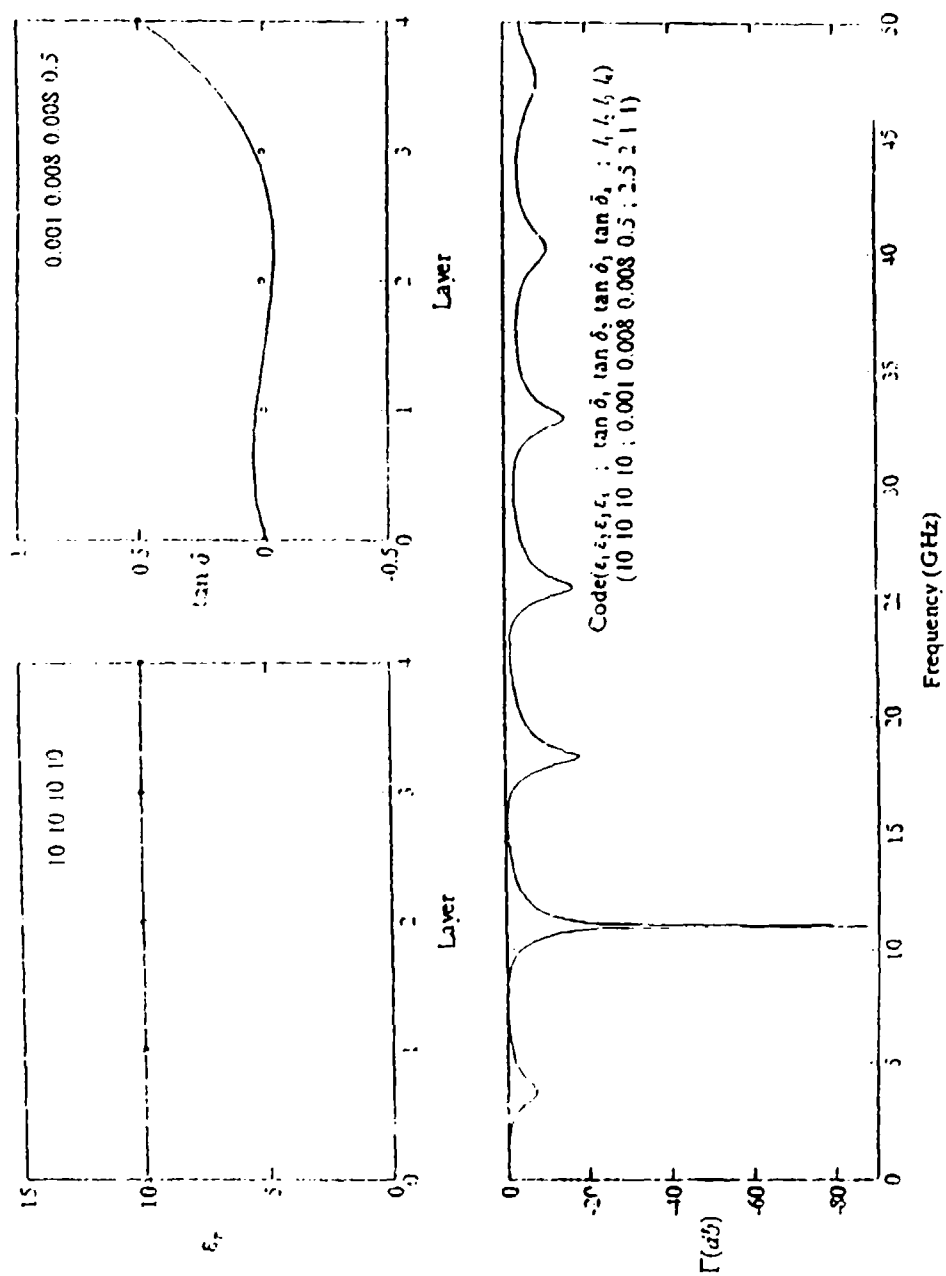


Figure 8. STRUCTURE WITH MINIMUM REFLECTION AT 11 GHz

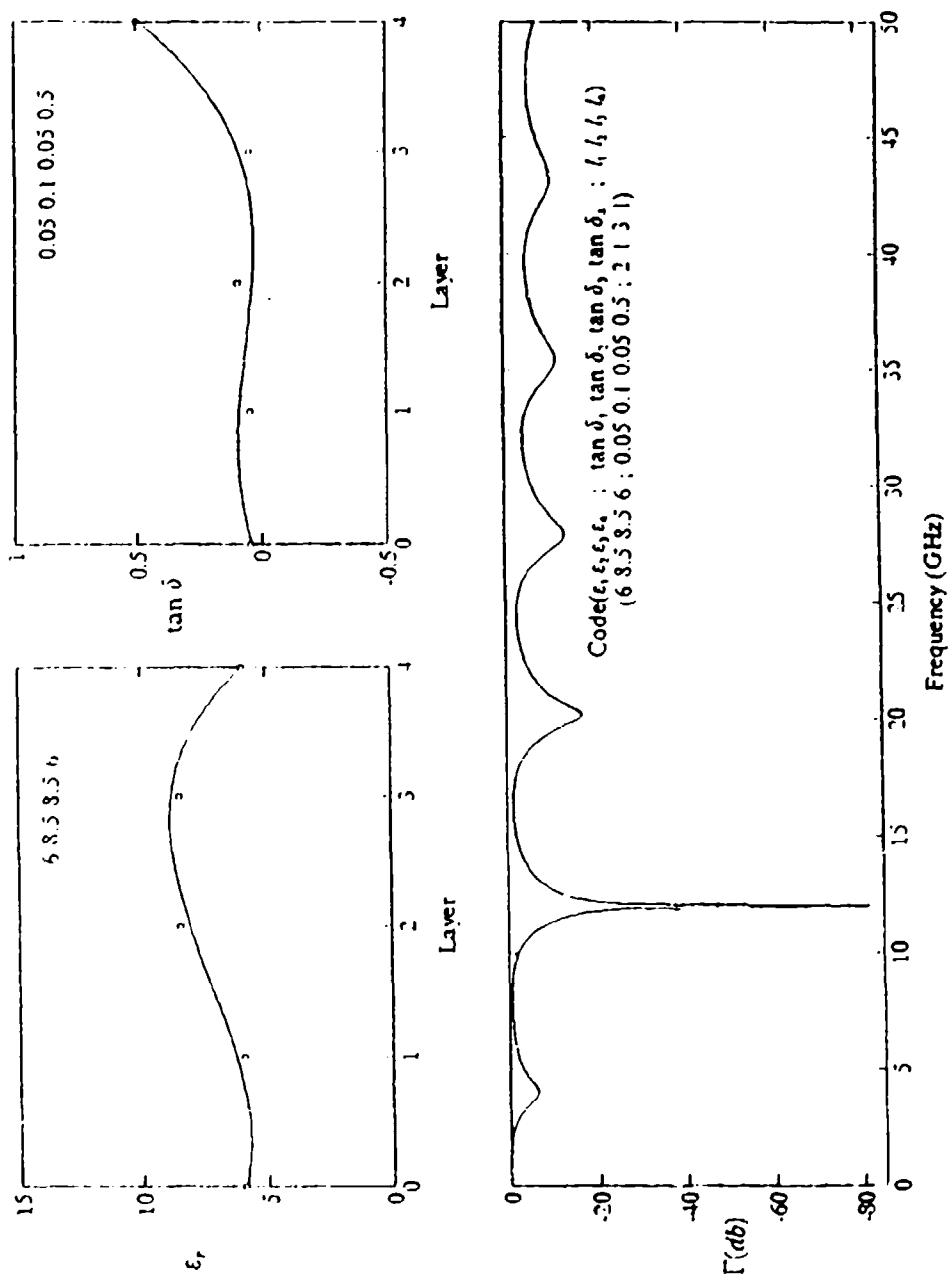


Figure 9. STRUCTURE WITH MINIMUM REFLECTION AT 12 GHz

C. SEARCH FOR LAYER STRUCTURES HAVING MINIMUM REFLECTION WITH BROAD BANDWIDTH

Although the narrow band absorber has a very low reflection coefficient at its fixed frequency, it is not desirable for military applications, because its narrow absorption bandwidth is not effective where hostile radar frequencies may have a range of values, or may be frequency-agile. In order to extend the absorption bandwidth, the computation of reflection coefficient was carried out using the absorption bandwidth $\Delta\Gamma$ (Eq.(2-10)) as a test parameter. Figures 10 and 14 to 19 show the absorption spectra of layer structures having low reflection over a broad bandwidth in the frequency range 1 to 50 GHz. These show reflection coefficients in dB units.

Standard radar detection theory [Ref. 13] shows that for a radar receiver operating at a signal to noise ratio (S/N) of 18 dB, the probability of detection will be essentially 100 % at a false alarm probability (PFA) of $1E-12$. If the S/N ratio is reduced by 10 dB, the probability of detection falls to well below 1%, at the same level of PFA. Although these are ideal values, a reflection coefficient of -12.5 dB may be taken in Figs.10 to 18 as a criterion of low radar-cross section. Table 4 summa-

performance of these structures under this criterion by definition of bandwidth (%) as,

$$B.W(\%) = 2 \frac{(f_{\max} - f_{\min})}{(f_{\max} + f_{\min})} \times 100 \quad (4 - 1)$$

Table 4. RCS PERFORMANCE OF BROADBAND STRUCTURES

Fig	Freq. range (GHZ)	ECM band	B.W (%)
10	12.1-26.7, 35-50	J , K	75.3
14	26.8-50	K , L	60.4
15	26.8-50	K , L	60.4
16	24.7-50	K , L	67.7
17	13.3-26.7, 41-50	J , K	67.0
18	7.6-50	H,I,J,K,L	147.1

The material constant distributions of the broad-banded layered RCS structures in Fig.10 above shows the characteristics of low relative dielectric constant at the air/layer interface, with rising ϵ , toward the metal backplane. It is interesting to note that these broad-bandwidth structures had the lowest value of loss tangent in the second layer from the air interface, and a generally have a smaller percentage variation of $\tan \delta$ among the layers than for the resonant structures of Figs.5 to 9.

The structures shown in Figs.11, 12 and 13 were derived from Figs.5, 6 and 9 by a changing only the relative dielectric constant but maintaining the same loss tangent profile as in Fig.10. It may be noted that the curves of Figs.11,12 and 13 are qualitatively similar in form to the narrow-band cases shown Figs. 5, 6 and 12 except for the reflection coefficient magnitude. Figures 14, 15 and 16 have the same dielectric profile as the narrowband profile of Figs.5, 6 and 9 respectively, except that the dielectric constant of the outermost layer is made unity in Figs.14,15 and 16. This structure leads to absorption of energy over a wide frequency range beyond 25GHz as shown in Figs.14, 15 and 16. In addition, placing the lowest value of relative dielectric constant at the second layer from the air interface, leads to a low reflection coefficient which extends from 13.3 GHz to 26.7 GHz and from 45 GHz to up, as shown in Fig.17. Although the lossy layer having unit value of relative dielectric permittivity which was cited above for the air-interface layer is an idealization, it is assumed that it could be approximated by a suitable porous compound containing lossy material, or in similar fashion. Figures 10 and 14 to 16 show that it is relatively easy to obtain low reflection over broad bandwidths at frequencies beyond 25 GHz. It is felt that future experimentation with layer parameter values can produce broader-

banded structures in the X-band and Ku-band regions. For example, placing the lower value of relative dielectric constant at the second layer from metal interface for the structure shown in Fig.18, led to a structure with a low reflection coefficient which extends from 7.6 GHZ to 50 GHZ as shown in Fig.18. This structure has the broadest absorption bandwidth which was found after only limited experimentation with the adjustment of layer parameter values. From these results it may be concluded that the broad-bandwidth structures have the common characteristics of low relative dielectric constant, (unit value), at the air/layer interface with increasing value to the metal /layer interface and having a lowest value of loss tangent in the second layer from air surface with smaller variation of its value among the layers than the resonant layers described in preceding section. In further research, additional trials should be made to produce broad-banded low- RCS structures by further adjustment of layer parameters as described above. It is assumed that there is potential for the production of additional high performance RAM structures, by the methods outlined.

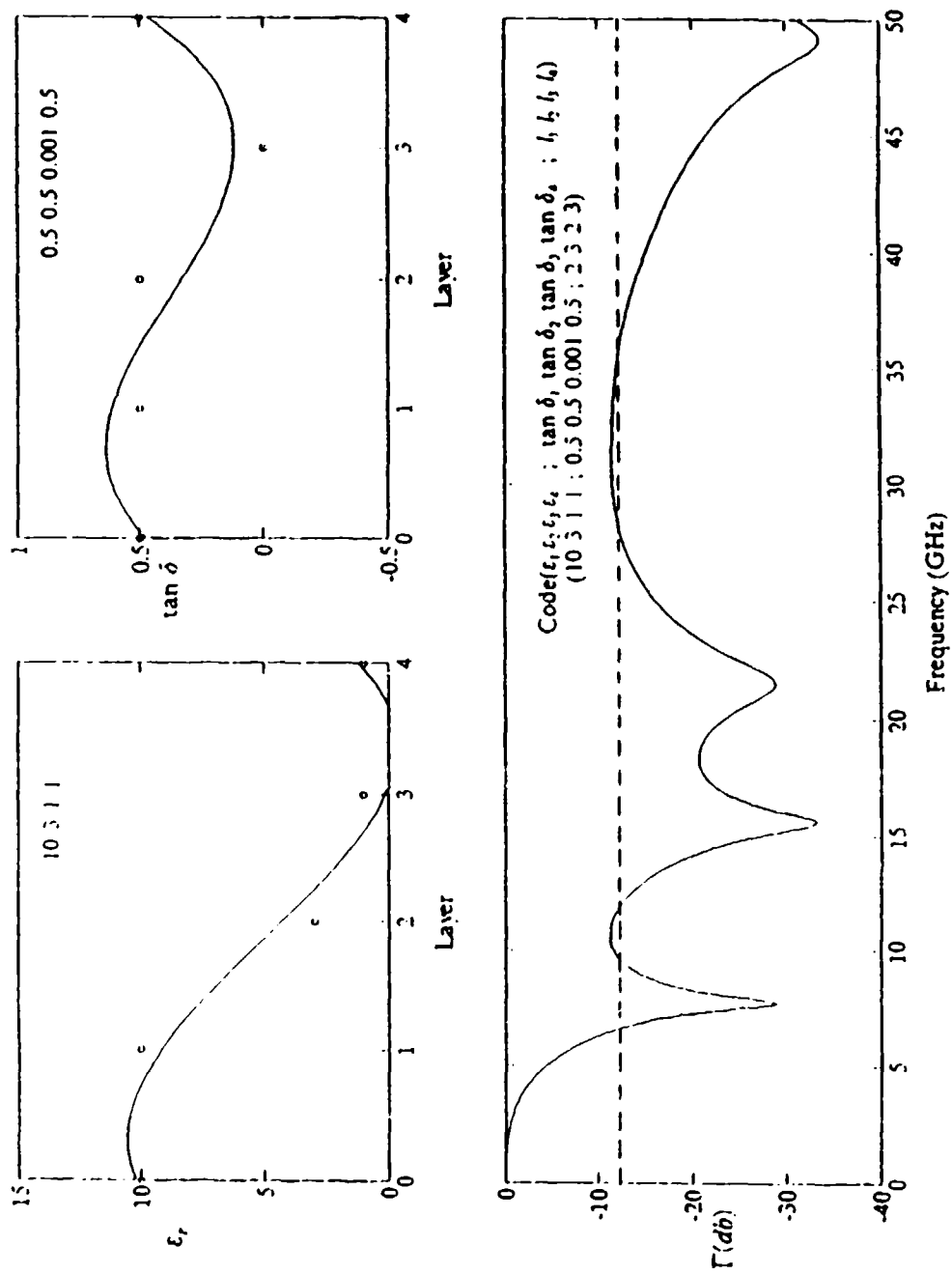


Figure 10. BROAD-BAND STRUCTURE RESPONSE

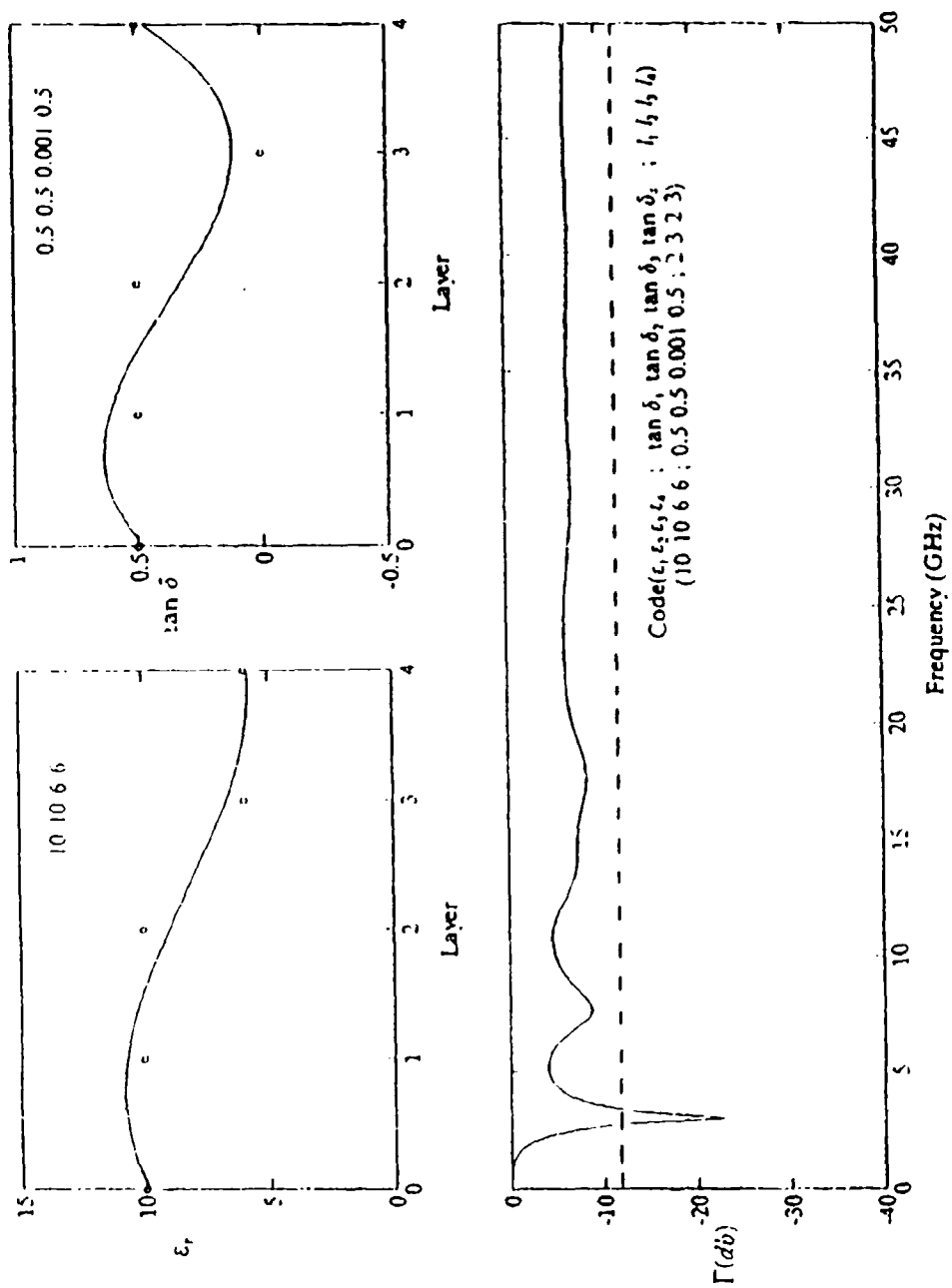


Figure 11. NARROW-BAND STRUCTURE RESPONSE DESIGNED FOR 8 GHz

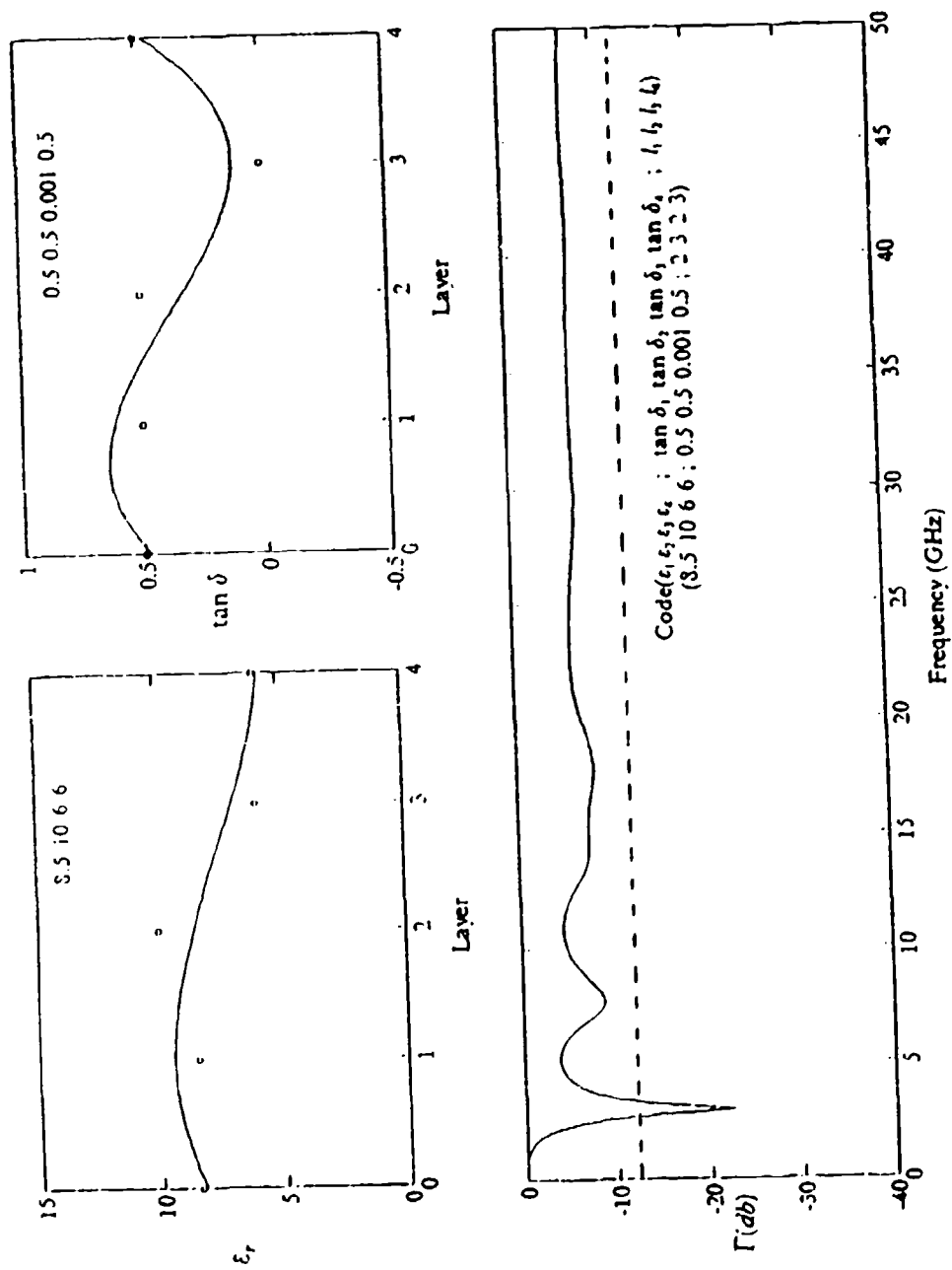


Figure 12. NARROW-BAND STRUCTURE RESPONSE DESIGNED FOR 9 GHz

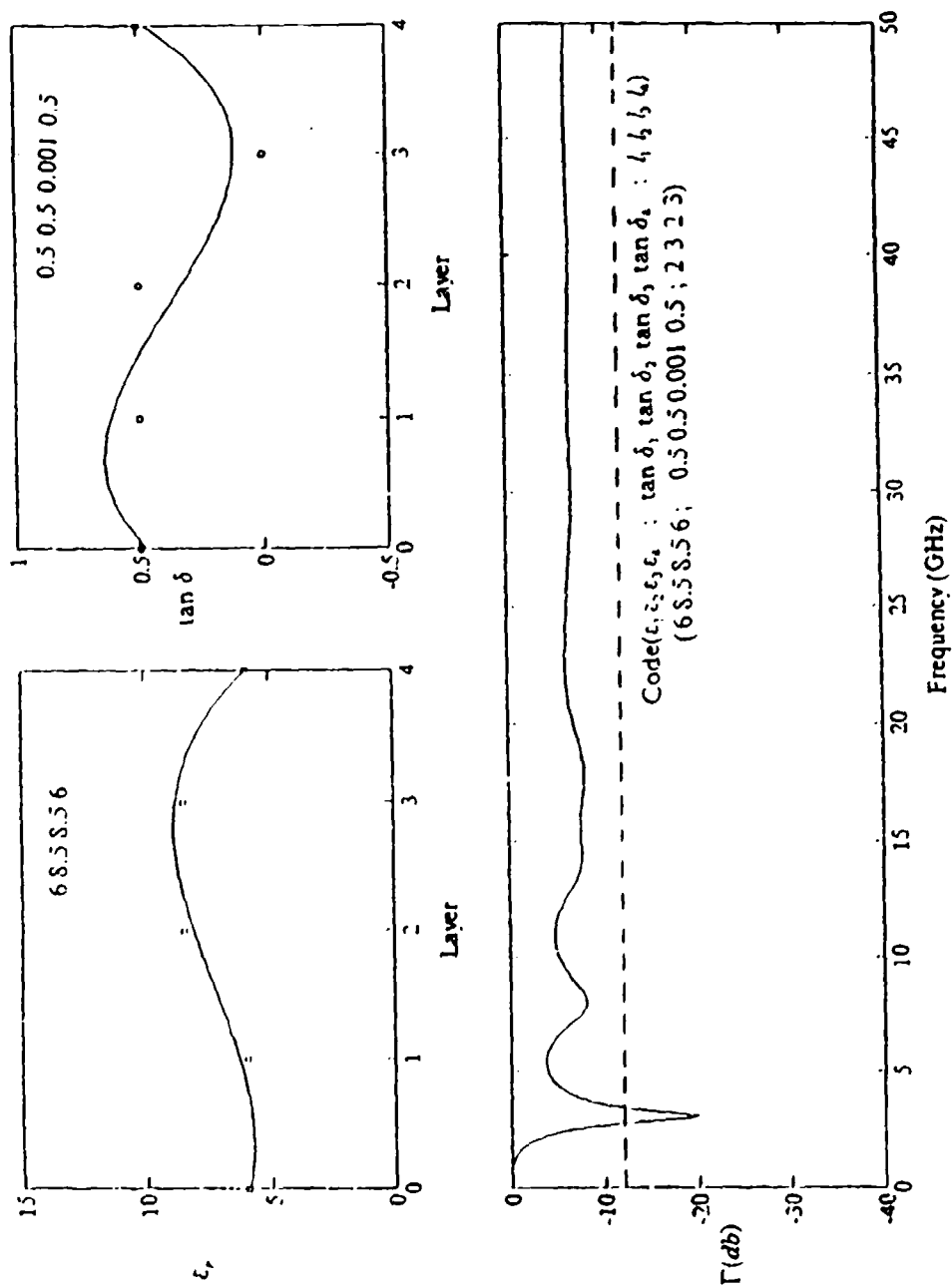


Figure 13. NARROW-BAND STRUCTURE RESPONSE DESIGNED FOR 12 GHz

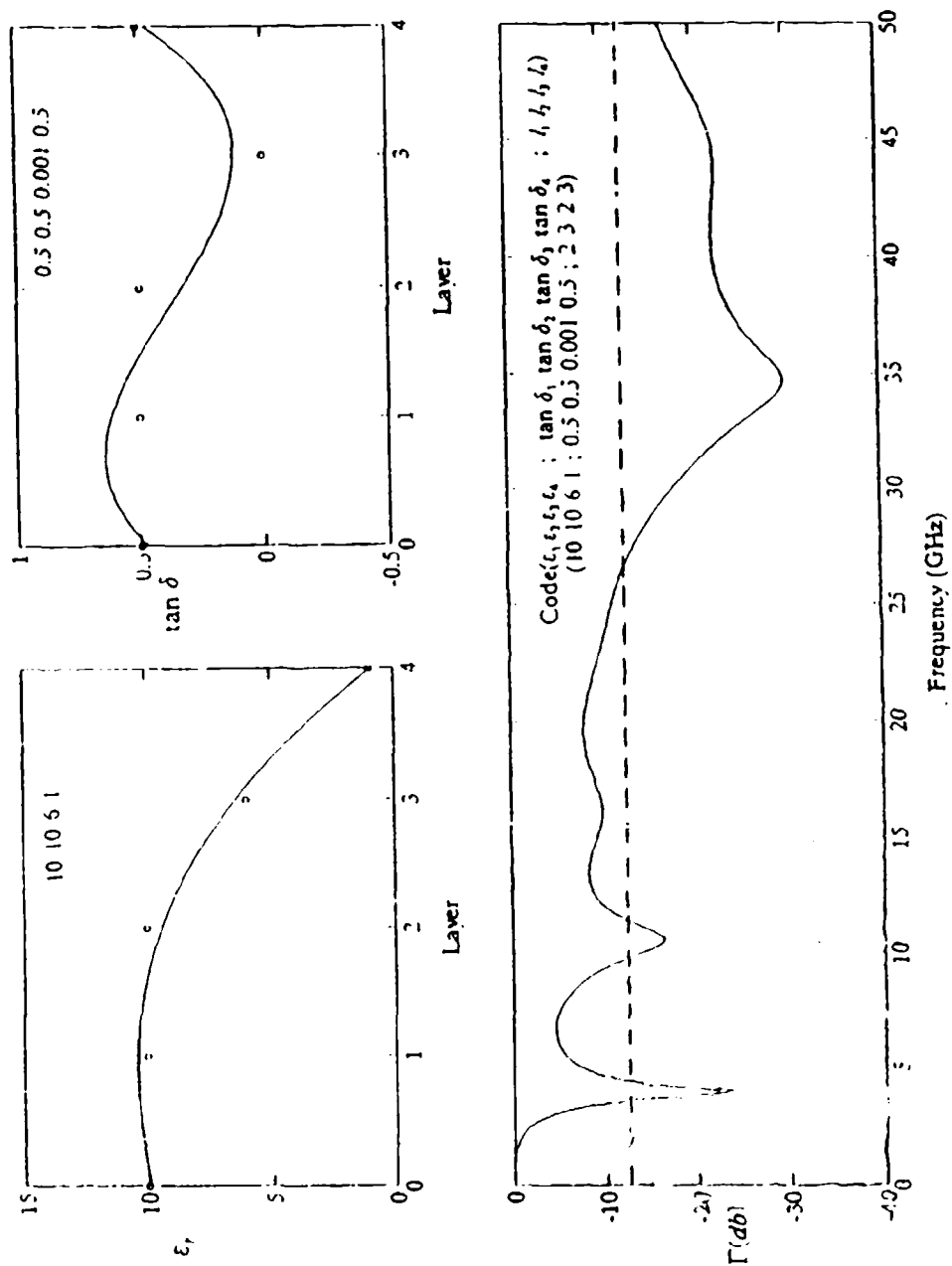


Figure 14. BROAD-BAND STRUCTURE RESPONSE

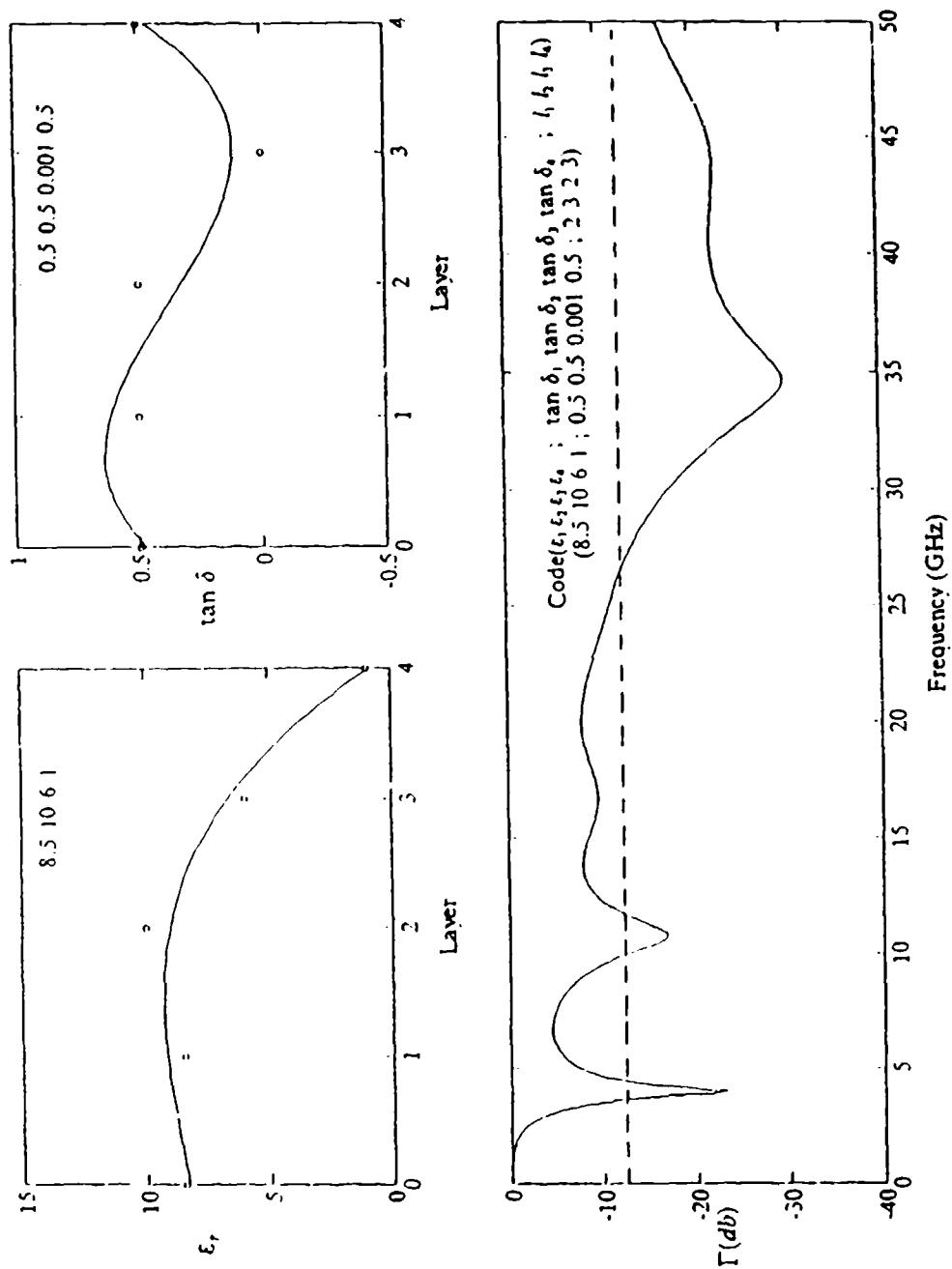


Figure 15. BROAD-BAND STRUCTURE RESPONSE

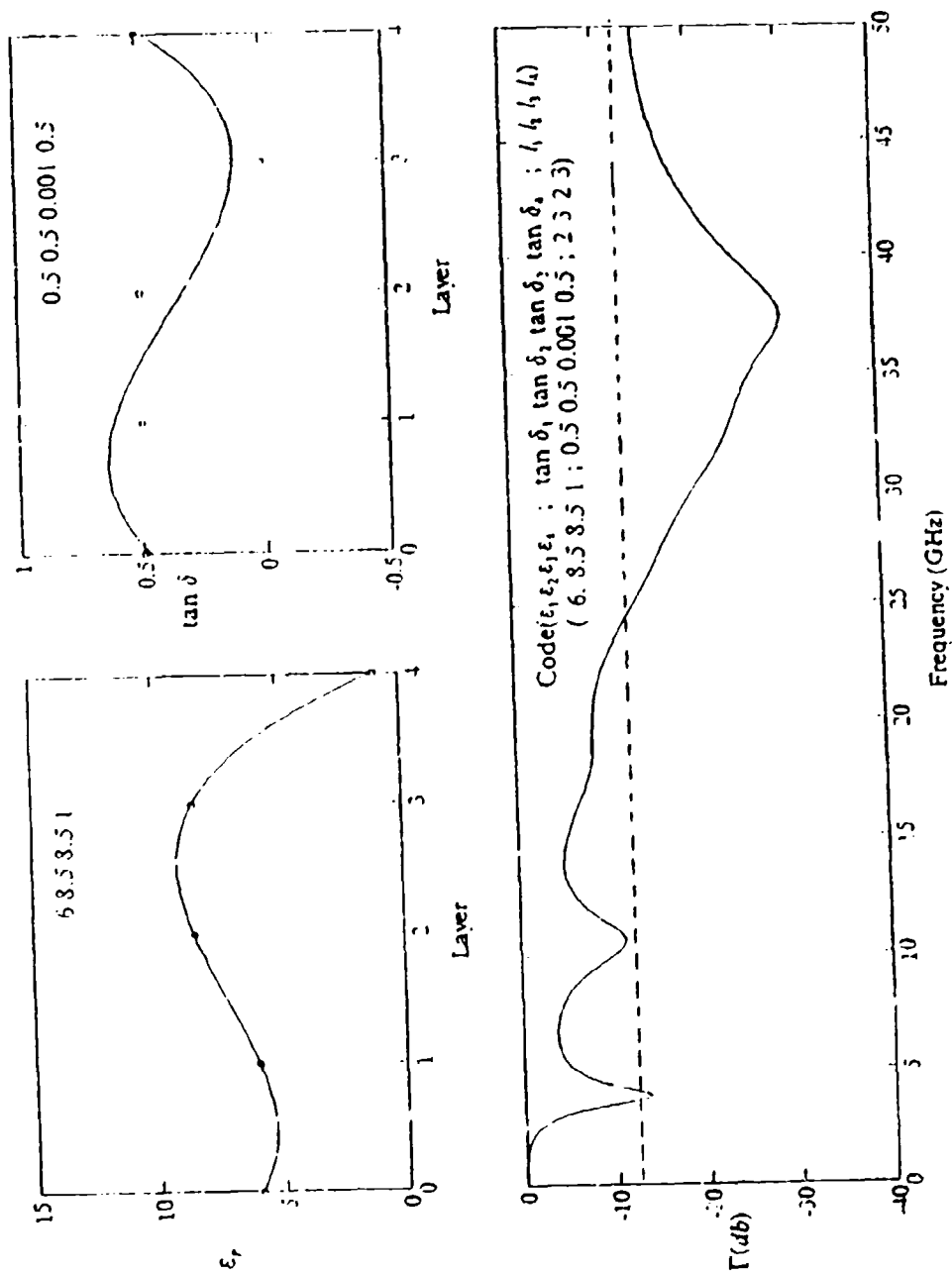


Figure 16. BROAD-BAND STRUCTURE RESPONSE

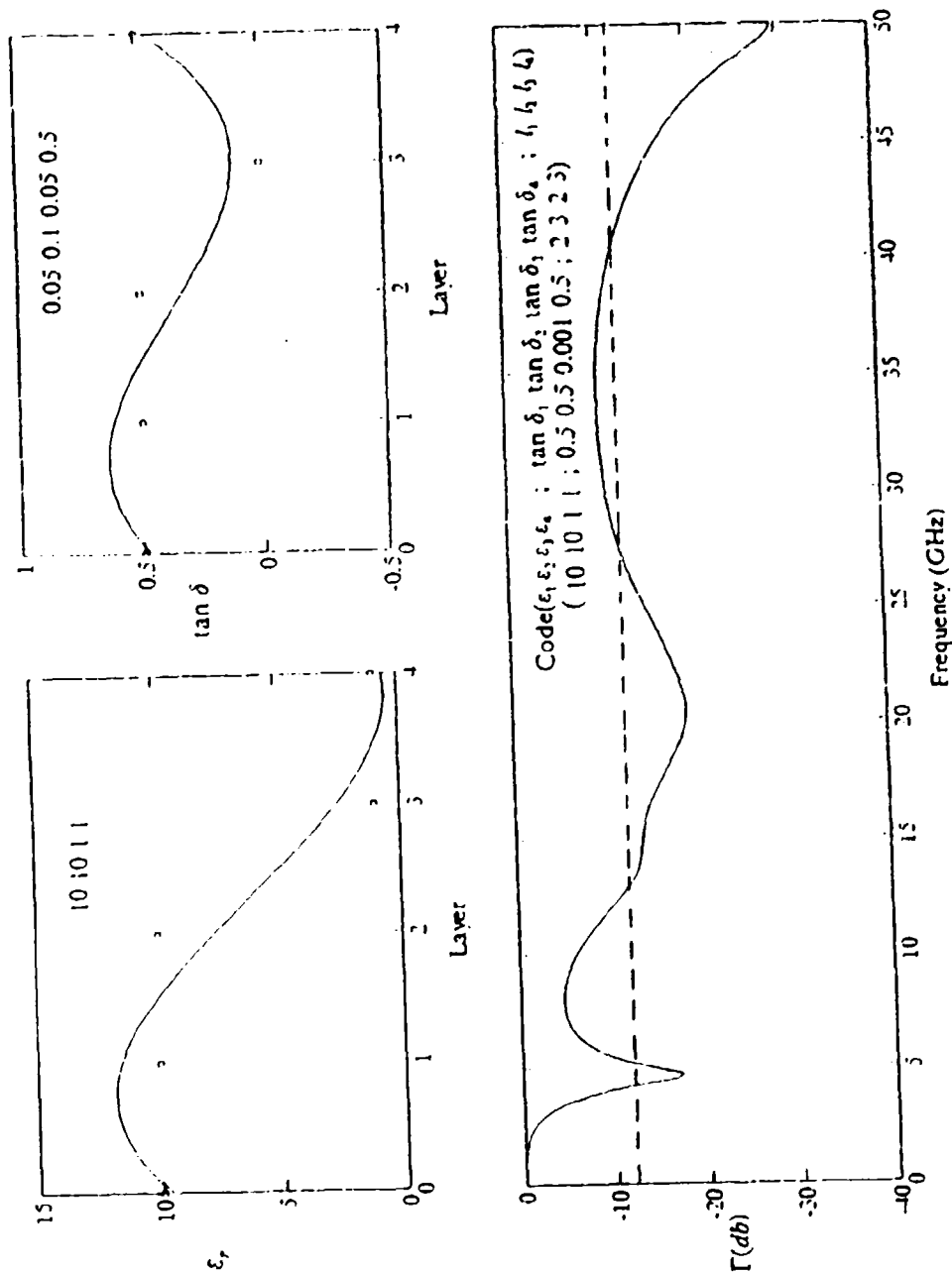


Figure 17. BROAD-BAND STRUCTURE RESPONSE

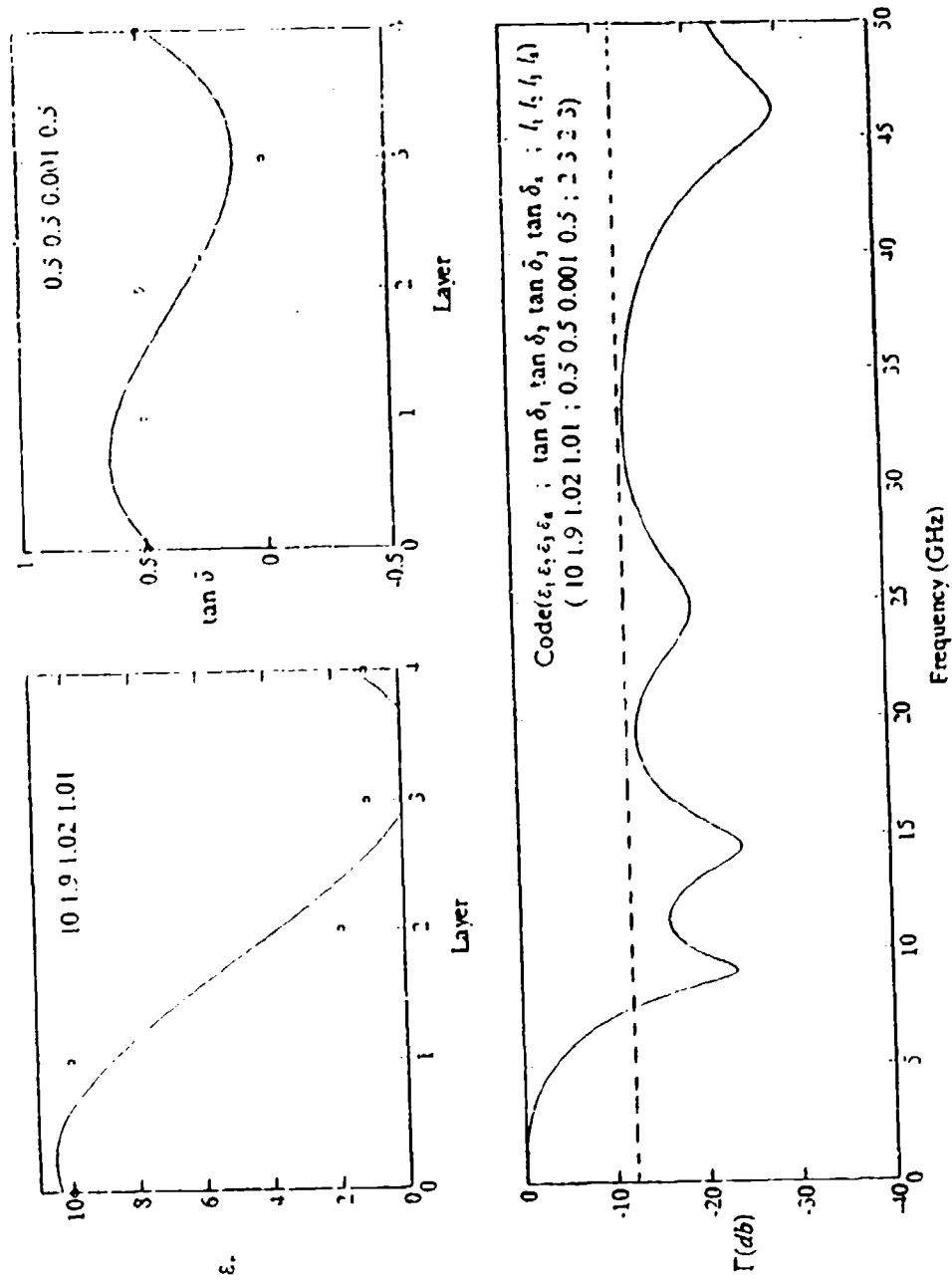


Figure 18. BROAD-BAND STRUCTURE RESPONSE

IV. CONCLUSION

Radar absorbing materials can make it possible to hide an incoming military vehicle by reducing the radar echo to a very low level. The radar cross section of an object may be reduced over a specific range of frequencies by applying to the surface of the object a material which absorbs the incident energy. Satisfactory broadband absorbing material performance depends on getting the RF energy into the RAM and then providing sufficient loss to absorb the necessary energy within the allowed RAM thickness. These two requirements often conflict, because high-loss materials often have intrinsic impedance much different from that of free space, and thus suffer high front face reflections. A simple solution of this for a single layer structure is to employ materials with both a high-loss and an intrinsic impedance near to that of free space. The present work was done under the constraint of using multilayered lossy dielectric materials to find best structure for both the fixed-frequency case and broadband case. Structures having a wide range of material parameters were scanned while retaining a maximum thickness of 1 cm.

The research found that broad absorption bandwidth structure calls for a typical distribution of the layer parameters: a variation with a high

value of dielectric constant near the metal backplane changing to a nearly unit value at the air/dielectric interface layer. In addition, the distribution of loss tangent should have its lowest value in the second layer from the air/layer interface. The use of multilayered dielectric materials i.e. non-ferrite based materials is capable of reducing the radio wave reflection over significant frequency ranges by suitable control of the distribution of the layer parameters of the structure.

APPENDIX A. COMPUTER PROGRAM

FOR

MINIMUM REFLECTION COEFF

THIS PROGRAM PROVIDES THE SCAN OF LAYER PARAMETERS AT FIXED FREQUENCY

```

DOUBLE PRECISION MINGAM,GAMA4
INTEGER N ,COUNT,I1,I2,I3,I4,J1,J2,J3,J4,K1,K2,K3,K4
REAL PI,E0,MUO,F1,OMG,ER(10),D(15),L(10),Z,V
COMPLEX JAY,EFF1,EFF2,EFF3,EFF4
COMPLEX THETA1,THETA2,THETA3,THETA4
COMPLEX ETA1,ETA2,ETA3,ETA4,D1,B1
COMPLEX A2,B2,C2,D2, A3,B3,C3,D3
COMPLEX SSH1,SSH2,CSH1,CSH2,SSH3,CSH3
COMPLEX SSH4,CSH4,A4,B4,C4,D4
COMPLEX GAMMA4,ZIN1,ZIN2,ZIN3,ZIN4
PI=4*ATAN(1.)
F1=9.
N=4
EO=(1E-9)/(36*PI)
OMG=2*PI*F1*1E9
MUO=PI*(4E-7)
JAY=CMPLX(0.,1.)
ER(1)=1.0
ER(2)=3.0
ER(3)=6.0
ER(4)=8.5
ER(5)=10.0
D(1)=0.001
D(2)=0.008
D(3)=0.05
D(4)=0.1
D(5)=0.5
L(1)=0.001
L(2)=0.002
L(3)=0.0025
L(4)=0.003
MINGAM=1.0
COUNT=1
WRITE(5,12)
WRITE(5,13)
12  FORMAT(1X,'MINGAMA',16X,'COUNT')
13  FORMAT(3X,'ER(1)',2X,'Q(1)',1X,'LI(1)',2X,'ER(2)',1X,'Q(2)'
+      ,1X,'LI(2)',2X,'ER(3)',2X,'Q(3)',1X,'LI(3)',2X,
+      'ER(4)',2X,'Q(4)',1X,'LI(4)')
DO 99 I1=1,5
DO 98 J1=1,5
DO 97 K1=1,4

```

```

DO 96 I2=1,5
DO 95 J2=1,5
DO 94 K2=1,4
DO 93 I3=1,5
DO 92 J3=1,5
DO 91 K3=1,4
DO 90 I4=1,5
DO 89 J4=1,5
DO 88 K4=1,4
  Z=L(K1)+L(K2)+L(K3)+L(K4)
  IF ((N.EQ.4).AND.(Z.LE.0.01)) THEN
    EFF1=ER(I1)*E0*(1-JAY*D(J1))
    THETA1=JAY*CSQRT(MU0*EFF1)*OMG*L(K1)
    SSH1=(CEXP(THETA1)-1/CEXP(THETA1))/2
    CSH1=(CEXP(THETA1)+1/CEXP(THETA1))/2
    ETA1=CSQRT(MU0/EFF1)
    D1=CSH1
    B1=ETA1*SSH1
    ZIN1=B1/D1
    EFF2=ER(I2)*E0*(1-JAY*D(J2))
    THETA2=JAY*CSQRT(MU0*EFF2)*OMG*L(K2)
    SSH2=(CEXP(THETA2)-1/CEXP(THETA2))/2
    CSH2=(CEXP(THETA2)+1/CEXP(THETA2))/2
    ETA2=CSQRT(MU0/EFF2)
    A2=CSH2
    D2=CSH2
    B2=ETA2*SSH2
    C2=SSH2/ETA2
    ZIN2=(A2*ZIN1+B2)/(C2*ZIN1+D2)
    EFF3=ER(I3)*E0*(1-JAY*D(J3))
    THETA3=JAY*CSQRT(MU0*EFF3)*OMG*L(K3)
    ETA3=CSQRT(MU0/EFF3)
    SSH3=(CEXP(THETA3)-1/CEXP(THETA3))/2
    CSH3=(CEXP(THETA3)+1/CEXP(THETA3))/2
    A3=CSH3
    B3=ETA3*SSH3
    C3=SSH3/ETA3
    D3=CSH3
    ZIN3=(A3*ZIN2+B3)/(C3*ZIN2+D3)
    EFF4=ER(I4)*E0*(1-JAY*D(J4))
    THETA4=JAY*CSQRT(MU0*EFF4)*OMG*L(K4)
    ETA4=CSQRT(MU0/EFF4)
    SSH4=(CEXP(THETA4)-1/CEXP(THETA4))/2
    CSH4=(CEXP(THETA4)+1/CEXP(THETA4))/2
    A4=CSH4
    B4=ETA4*SSH4
    C4=SSH4/ETA4
    D4=CSH4
    ZIN4=(A4*ZIN3+B4)/(C4*ZIN3+D4)
    GAMMA4=((ZIN4-377.)/(ZIN4+377.))
    GAMA4=CABS(GAMMA4)
    IF (MINGAM.GT.GAMA4) THEN
      MINGAM=GAMA4
      WRITE(5,43) MINGAM,COUNT
      WRITE(5,44) ER(I1),D(J1),L(K1),ER(I2),
        D(J2),L(K2),ER(I3),D(J3),L(K3)

```

```

      +
43      ,ER(I4),D(J4),L(K4)
44      FORMAT(1X,F18.16,2X,I6)
      FORMAT(1X,4(F6.3,1X,F5.4,1X,F5.4,1X))
      COUNT=COUNT+1

      ELSE

      V=GAMA4-MINGAM
      IF((V.NE.0.).AND.(V.LE.1E-3)) THEN
      WRITE(5,73) GAMA4
      WRITE(5,74) ER(I1),D(J1),L(K1),ER(I2)
      ,D(J2),L(K2),ER(I3),D(J3)
      ,L(K3),ER(I4),D(J4),L(K4)
      73      FORMAT(1X,F18.16)
      74      FORMAT(1X,4(F6.3,1X,F5.3,1X,F5.4,1X))
      ENDIF

      ENDIF

      CONTINUE
88      CONTINUE
89      CONTINUE
90      CONTINUE
91      CONTINUE
92      CONTINUE
93      CONTINUE
94      CONTINUE
95      CONTINUE
96      CONTINUE
97      CONTINUE
98      CONTINUE
99      CONTINUE
      STOP
      END

```

APPENDIX B. COMPUTER PROGRAM TO SEARCH FOR BROAD ABSORPTION BANDWIDTHS

THIS PROGRAM IS DESIGNED, TO FIND BROAD ABSORPTION BANDWIDTHS BY
USING BANDWIDTH PARAMETER.

```

DOUBLE PRECISION MINGAM ,GAM(500),F(500)
DOUBLE PRECISION FREQ ,FIG,DELGAM
INTEGER N,M,O,V,JMIN,COUNT
REAL PI,E0,MU0,OMG,ER(5),D(5),L(4),Z
COMPLEX JAY,EFF1,EFF2,EFF3,EFF4
COMPLEX THETA1,THETA2,THETA3,THETA4
COMPLEX ETA1,ETA2,ETA3,ETA4,D1,B1
COMPLEX A2,B2,C2,D2, A3,B3,C3,D3
COMPLEX SSH1,SSH2,CSH1,CSH2,SSH3,CSH3
COMPLEX SSH4,CSH4,A4,B4,C4,D4
COMPLEX GAMMA4,ZIN1,ZIN2,ZIN3,ZIN4
C OPEN(UNIT=6,FILE='THE1')
PI      = 4*ATAN(1.)
N       = 4
E0      = (1E-9)/(36*PI)
MU0     = PI*(4E-7)
JAY     = CMPLX(0.,1.)
MINFIG  = 1.0
COUNT  = 1
WRITE(6,12)
WRITE(6,13)
12  FORMAT(1X,'GAMMIN',8X,'DELGAM',17X,'FREQ',16X,'FIG',10X,'V')
13  FORMAT(3X,'ER(1)',2X,'Q(1)',1X,'LI(1)',2X,'ER(2)',1X,'Q(2)'
+      ,1X,'LI(2)',2X,'ER(3)',2X,'Q(3)',1X,'LI(3)',2X,
+      'ER(4)',2X,'Q(4)',1X,'LI(4)')
ER(1)   = 10.
ER(2)   = 8.5
ER(3)   = 6.
ER(4)   = 3.0
ER(5)   = 1.0
D(1)    = 0.001
D(2)    = 0.008
D(3)    = 0.5
D(4)    = 0.001
D(5)    = 0.5
L(1)    = 0.001
L(2)    = 0.002
L(3)    = 0.0025
L(4)    = 0.003
DO 99 I1 = 1,1
  DO 98 J1 = 3,3
    DO 97 K1 = 1,4
      DO 96 I2 = 1,5

```



```

DO 95 J2 = 1,5
DO 94 K2 = 1,4
DO 93 I3 = 1,5
DO 92 J3 = 1,5
DO 91 K3 = 1,4
DO 90 I4 = 1,5
DO 89 J4 = 1,5
DO 88 K4 = 1,4
Z = L(K1)+L(K2)+L(K3)+L(K4)
IF ((N.EQ.4).AND.(Z.LE.0.01)) THEN
DO 87 FREQ=8.0D0,1.3D1,1.0D0
OMG = 2*PI*FREQ*1E9
O = COUNT
F(0) = FREQ
EFF1 = ER(I1)*EO*(1-JAY*D(J1))
THETA1 = JAY*CSQRT(MUO*EFF1)*OMG*L(K1)
SSH1 = (CEXP(THETA1)-1/CEXP(THETA1))/2
CSH1 = (CEXP(THETA1)+1/CEXP(THETA1))/2
ETA1 = CSQRT(MUO/EFF1)
D1 = CSH1
B1 = ETA1*SSH1
ZIN1 = B1/D1
EFF2 = ER(I2)*EO*(1-JAY*D(J2))
THETA2 = JAY*CSQRT(MUO*EFF2)*OMG*L(K2)
SSH2 = (CEXP(THETA2)-1/CEXP(THETA2))/2
CSH2 = (CEXP(THETA2)+1/CEXP(THETA2))/2
ETA2 = CSQRT(MUO/EFF2)
A2 = CSH2
D2 = CSH2
B2 = ETA2*SSH2
C2 = SSH2/ETA2
ZIN2 = (A2*ZIN1+B2)/(C2*ZIN1+D2)
EFF3 = ER(I3)*EO*(1-JAY*D(J3))
THETA3 = JAY*CSQRT(MUO*EFF3)*OMG*L(K3)
ETA3 = CSQRT(MUO/EFF3)
SSH3 = (CEXP(THETA3)-1/CEXP(THETA3))/2
CSH3 = (CEXP(THETA3)+1/CEXP(THETA3))/2
A3 = CSH3
B3 = ETA3*SSH3
C3 = SSH3/ETA3
D3 = CSH3
ZIN3 = (A3*ZIN2+B3)/(C3*ZIN2+D3)
EFF4 = ER(I4)*EO*(1-JAY*D(J4))
THETA4 = JAY*CSQRT(MUO*EFF4)*OMG*L(K4)
ETA4 = CSQRT(MUO/EFF4)
SSH4 = (CEXP(THETA4)-1/CEXP(THETA4))/2
CSH4 = (CEXP(THETA4)+1/CEXP(THETA4))/2
A4 = CSH4
B4 = ETA4*SSH4
C4 = SSH4/ETA4
D4 = CSH4
ZIN4 = (A4*ZIN3+B4)/(C4*ZIN3+D4)
GAMMA4 = ((ZIN4-377.)/(ZIN4+377.))
GAM(0) = CABS(GAMMA4)
COUNT = COUNT+1

```

CONTINUE

```

45      DO 100 M = 2 , (O-1)
      IF ((GAM(M). LT. GAM(M-1)). AND.
+      (GAM(M). LT. GAM(M+1))) THEN
          JMIN = M
          MINGAM = GAM(JMIN)
          DELGAM=((GAM(JMIN-1)-GAM(JMIN))+(GAM(JMIN+1)-GAM(JMIN)))/2
          IF ((LOG10(MINGAM). LE. -1. 0). AND.
+ (LOG10(DELGAM). LE. -1. 3)) THEN
              FIG = LOG10(MINGAM)+LOG10(DELGAM)
              IF (FIG. LE. MINFIG) THEN
                  MINFIG=FIG
                  V=1
              ELSE
                  V=0
              *   ENDIF
              WRITE(6,43) MINGAM,DELGAM,F(JMIN),FIG,V
              WRITE(6,44) ER(I1),D(J1),L(K1),ER(I2),D(J2),L(K2)
+ ,ER(I3),D(J3),L(K3),ER(I4),D(J4),L(K4)
93      FORMAT(1X,F10. 8,2X,F20. 15,2X,F13. 8,6X,F15. 8,4X,I2)
94      FORMAT(1X,4(F6. 3,1X,F5. 4,1X,F5. 4,1X))
              ENDIF
100      CONTINUE
          COUNT=1
          ENDIF
88      CONTINUE
89      CONTINUE
90      CONTINUE
91      CONTINUE
92      CONTINUE
93      CONTINUE
94      CONTINUE
95      CONTINUE
96      CONTINUE
97      CONTINUE
98      CONTINUE
99      CONTINUE
C      PRINT*, 'LOG10(MINGAM)=', LOG10(MINGAM), 'DLO=', LOG10(DELGAM)
C      PRINT*, 'LOGMI=', LOG10(MINGAM), 'LDEL=', LOG10(DELGAM)
C      PRINT*, 'MINGAM=', MINGAM, 'DELGAM=', DELGAM
      STOP
      END

```

LIST OF REFERENCES

1. D.C. Schleher, *Introduction to Electronic Warfare*, Artech House, Norwood, Massachusetts, pp.534 - 537, 1986.
2. E.F.Knott, J.F.Shaeffler, M.T.Tuley, *Radar Cross Section*, Artech House, Norwood, Massachusetts, pp.198 - 218, 1988.
3. Y.Shimizu and K.Suetake, *Minimum-Thickness Design of Broad-Band Absorbing Wall*, Trans. I.E.C.E., Japan, Vol. 51B, No.3, pp.57 - 63 (1968).
4. R.N.Johnson, *Radar Absorbing Materials Passive Role in An Active Scenario*, International Countermeasures Handbook, pp.375 - 381(1986).
5. M.Skolnik, *Radar Handbook*, McGraw-Hill, New York, pp.11.43 - 11.56, 1962.
6. M.B.Amin, and J.R.James, *Techniques for Utilization of Hexagonal Ferrites in Radar Absorbers: Part 1, Broadband Planar Coatings*, The Radar and Electronic Engineer, Vol.51, No.5, pp.209 - 218, May, 1981.
7. B.Lax, and K.J.Button, *Microwave Ferrites and Ferrimagnetics*, McGraw-Hill, New York, pp.297 - 322, 1962.

8. D.K.Cheng, *Field and Wave Electromagnetics*, Addison Wesley, New York, pp.332 - 406, 1989.
9. H.A.Atwater, *Introduction to Microwave Theory*, Krieger, Malabar, pp.24 - 46, 1981.
10. R.G.Brown, R.A.Sharpe, W.L.Hughes, and R.E.Post, *Lines, Waves, and Antennas*, Wiley, New York, pp.177 - 210, 1973.
11. P.A.Rizzi, *Microwave Engineering: Passive Circuits*, Prentice Hall, Englewood Cliffs, New Jersey, pp.534 - 545, 1988.
12. A.V.Hippel, *Dielectric Materials and Applications*, Wiley, New York, pp.301 - 370, 1954.
13. M.Skolnik, *Introduction to Radar Systems*, McGraw-Hill, New York, pp.20 - 29, 1980.

INITIAL DISTRIBUTION LIST

	No. Copies
1. Defense Technical Information Center Cameron Station Alexandria, VA 22304-6145	2
2. Library, Code 52 Naval Postgraduate School Monterey, CA 93943-5002	2
3. Prof. Harry A. Atwater, Code EC/AN Department of Electrical and Computer Engineering Naval Postgraduate School Monterey, CA 93943 - 5002	1
4. Prof. Ramakrishna Janaswamy, Code EC/JS Department of Electrical and Computer Engineering Naval Postgraduate School Monterey, CA 93943 - 5002	1
5. Library of the Naval Academy Angogok Dong, Chinhae City, Gyungnam 602-00 Republic of Korea	2
6. Go, Han Suk 104dong 1006ho Hyundae APT. Yeomju DongSeogu, Kwangju City Republic of Korea	4
7. Cdr.Uwe Becker c/o Federal Republic of Germany Military Representative, sl-pers.o.V.I.A. 4000 Brandywine St., N.W. Washington, D.C 20016-1887	1

- | | | |
|-----|---|---|
| 8. | Cdr Chen-Kuo Yu
4F-2,282,Tung-Men Rd.
Ku-San, Kaohsing,
Taiwan 80401 Republic of China | 1 |
| 9. | Cdr.Harry Thornberry
Clemente x 335
San isidro
Lima
Peru | 1 |
| 10. | Maj.Won Tae Jin
#5-205 Misung APT.
Hong-Eun 3Dong
Sedaemoon-Ku
Seoul
Republic of Korea | 1 |
| 11. | Ltcdr.Geraldo Batista
Rua Alferes Esteves,313
356660 Para de Minas-MG
Brazil | 1 |
| 12. | Ltcdr. Carlos Augusto Teixeira
Rua Farani 60-A.P.904
Rio de Janeiro-RJ
Brazil | 1 |
| 13. | Ltcdr. Sudjiwo
Kompleks Tni-A1 No.178
Radio Dalam
Kebayoran Baru
Jakarta-Selatan.12140
Indonesia | 1 |
| 14. | Ltcdr.Ramesh Kumar
B-5-22
Nausanrakshan Society
NearLiberty Gaoen
Malao West Bombay, India | 1 |

- | | | |
|-----|--|---|
| 15. | Ltcdr.Kamran Kahn
1-C-4/11
Nazimabad
Karachi
Pakistan | 1 |
| 16. | Capt. Hyung Suk Kim
1651-2, Hwabuk 1 Dong
Jeju City
Jeju
Republic of Korea | 1 |
| 17. | Lt Jg. Levent Kurtoglu
Bulbuldere Cad.
Lalezar Ap.583
Kucukesat/Ankara
Turkey | 1 |
| 18. | Lt.Juan Jose Sanchez
Calle 3, No.46. Ota Lidice
Urb. Chucho Briceno
(1a Etapa), Cp.3002
Cabudare Edo.Lara
Venezuela | 1 |
| 19. | Lt.Mauricio Gaviria
Calle 71 #4-47
Bogota.DE
Colombia,S.A. | 1 |